LAWRENCE
LIVERMORE
NATIONAL
LABORATORY

LLNL-JRNL-409009

Effect of Reducing Groundwater on the Retardation of Redox-Sensitive Radionuclides

Qinhong Hu, mavrik zavarin, timothy p rose

November 25, 2008

geochemical transactions

Disclaimer

Effect of reducing groundwater on the retardation of redox-sensitive radionuclides

Qinhong Hu[1, 2*], Mavrik Zavarin[3], and Timothy P. Rose[3]

[1] College of Water Sciences, Beijing Normal University, Xinjiekouwai Street 19, Beijing 100875, P.R. China

[2] Department of Earth and Environmental Sciences, The University of Texas at Arlington, Arlington, TX 76019, USA

[3] Lawrence Livermore National Laboratory, 7000 East Avenue, MS L-231, Livermore, CA 94550, USA

Prepared for

Geochemical Transactions

May 16, 2008

[*]Corresponding author (phone: +1 925 784 5110; fax: +1 925 422 3160; E-mail address: huqinhong@yahoo.com)

Abstract

Laboratory batch sorption experiments were used to investigate variations in the retardation behavior of redox-sensitive radionuclides. Water-rock compositions used during these experiments were designed to simulate subsurface conditions at the Nevada Test Site (NTS), where a suite of radionuclides were deposited as a result of underground nuclear testing. Experimental redox conditions were controlled by varying the oxygen content inside an enclosed glove box and by adding reductants into the testing solutions. Under atmospheric (oxidizing) conditions, the radionuclide distribution coefficients varied with the mineralogical composition of the sorbent and the water chemistry. Under reducing conditions, distribution coefficients showed marked increases for ^{99}Tc and ^{237}Np in devitrified tuff, but much smaller variations in alluvium, carbonate rock, and zeolitic tuff. This effect was particularly important for ^{99}Tc, which tends to be mobile under oxidizing conditions. Unlike other redox-sensitive radionuclides, iodine sorption may *decrease* under reducing conditions when I^- is the predominant species. Overall, sorption of U to alluvium, devitrified tuff, and zeolitic tuff under atmospheric conditions was less than in the glove-box tests. However, the mildly reducing conditions achieved here were not likely to result in substantial U(VI) reduction to U(IV). Sorption of Pu was not affected by the decreasing redox conditions achieved in this study, as the predominant sorbed Pu species in all conditions was expected to be the low-solubility and strongly sorbing $Pu(OH)_4$. Depending on the aquifer lithology, the occurrence of reducing conditions along a groundwater flowpath could potentially contribute to the retardation of redox-sensitive radionuclides ^{99}Tc and ^{237}Np, which are commonly identified as long-term dose contributors in the risk assessment in various nuclear facilities.

Introduction

Major sources of radioactive waste and contamination include the production of nuclear fuels for the weapons program and electricity generation, nuclear weapons tests, fuel reprocessing, and nuclear accidents. In the United States, the total volume of all radioactive waste is 5.5 million m^3, with a total activity of about 1.2×10^9 TBq (tera becquerel; 1 TBq=27.03 Ci) [1]. In addition, there are large volumes of radiologically contaminated soil (30–80 million m^3) and water (1,800–4,700 million m^3), especially at U.S. Department of Energy (DOE) facilities that were used for weapons production [2]. The Nevada Test Site (NTS) is one such DOE facility, with substantial radiologic contamination resulting from nuclear weapons testing and abutting the proposed Yucca Mountain geological repository for high-level nuclear waste, which has been the focus of radionuclide transport investigations for more than three decades.

Numerous long-lived radionuclides are present in groundwater at the NTS as a result of 828 underground nuclear weapons tests conducted between 1951 and 1992. When weapons testing ended in September 1992, a total of about 4.9×10^6 TBq of radioactivity was present in the subsurface [3]. Important radionuclides, in terms of abundance, half-life, environmental mobility, and health effects, include ^{3}H (tritium), ^{14}C (carbon), ^{36}Cl (chlorine), ^{90}Sr (strontium), ^{99}Tc (technetium), ^{129}I (iodine), ^{137}Cs (cesium), ^{237}Np (neptunium), as well as isotopes of uranium (U), plutonium (Pu), and americium (Am). These radionuclides have been commonly identified as the set of contaminants that would cause risk to human health and the environment within the time frame of interest (1,000 years) for the environmental monitoring program at the NTS [4]. Among them, ^{3}H, ^{14}C, ^{36}Cl, ^{99}Tc, and ^{129}I presumably have large migration potential due to an assumed lack of interaction with the subsurface media.

The objective of the laboratory study described below is to use batch sorption experiments to investigate the impact of groundwater redox conditions on the mobility of selected radionuclides. Thus far, laboratory sorption data acquired for the radionuclide transport at the NTS has been based upon experiments conducted under atmospheric (oxidizing) conditions mainly because of the simplicity of the tests; this is also true for nearly all publications involving sorption measurements. For this investigation, we conducted a series of batch studies to evaluate the sorption behavior of redox-sensitive radionuclides (Tc, I, U, Np and Pu) under a range of redox conditions spanning those observed in NTS monitoring wells. Some radionuclides that are not redox-sensitive (e.g., Sr and Cs) were also included for comparison. The experiments were conducted using four different types of aquifer materials (alluvium, carbonate, devitrified tuff, and zeolitic tuff). Batch sorption experiments were conducted under atmospheric (oxidizing) conditions and in a glove box under five different controlled redox conditions spanning the range from oxidizing to moderately reducing.

Background

When studying field-scale radionuclide transport, a distribution coefficients (K_d) approach has been commonly employed to quantify the extent of radionuclide-aquifer-groundwater interaction. Values of K_d are used in transport simulations to empirically describe radionuclide/aquifer interactions that are the source of retardation for sorbing radionuclides. The K_d data are commonly determined from laboratory-scale batch and column experiments under oxidizing conditions [5] or computed by upscaling mechanistic processes [6].

Table 1 shows the range in measured K_d values for eight radionuclides for representative geologic media, including alluvium, carbonate rock, and volcanic tuffs (devitrified, vitric, and zeolitic) encountered at the NTS [4]. Generally speaking, the largest distribution coefficients are observed in the zeolitic tuff and in alluvium, and the smallest values in vitric tuff. Sorption of Pu

and Am onto carbonate rock is appreciable, and Np sorption on the carbonate is higher than other rock types (Table 1).

The K_d values for Tc and I in Table 1 are based on the assumption that pertechnetate (TcO_4^-) and iodide (I^-) are the dominant species in groundwater and during experimental measurements [5]. However, these and several of the other radionuclides listed in Table 1 (i.e., Tc, I, Np, U, and Pu) are redox-sensitive, and the speciation and retardation of these radionuclides is sensitive to their oxidation state. Variations in groundwater redox conditions, and associated changes in retardation factors are of particular importance to presumably mobile radionuclides, such as ^{99}Tc; reducing conditions could result in much longer transport times than those predicted with minimal retardation (i.e., K_d close to zero).

Geochemistry and sorption behavior of redox-sensitive radionuclides

Technetium-99

Technetium exists in valence states ranging from +7 to -1, but in natural environments the most stable valence states are +7 and +4 under oxidizing and reducing conditions, respectively. Technetium forms a reduced species [predominantly Tc(IV)] at redox potential (Eh) values below about 220 mV with respect to standard hydrogen electrode (SHE) in neutral pH conditions (Figure 1a). At higher Eh, it occurs as $Tc(VII)O_4^-$. Due to its weak interaction with mineral surfaces, TcO_4^- is considered as one of the most mobile radionuclides in the environment. In contrast, lower-valence Tc(IV) species [such as $TcO_2 \cdot nH_2O$ with n=1–2; equivalent to $TcO(OH)_2$ in Figure 1a when n=1] are expected to be strongly retarded due to their strong sorption and/or precipitation; the solubility of $TcO_2 \cdot nH_2O$(s) in carbonate-containing groundwater was reported to be about 10^{-8} M [7].

The presence of reductants in the host rock (e.g., Fe(II) in pyrite FeS_2) can contribute to the reduction of Tc(VII) to Tc(IV) [8]. For example, reducing groundwater was observed in boreholes on or near Yucca Mountain, in the western part of the NTS, several of which are known to contain pyrite [9]. Under reducing conditions, Cui and Eriksen [10-11] reported that TcO_4^- was reduced to $TcO_2 \cdot nH_2O(s)$ by Fe(II)-bearing fracture-filling minerals on which $Tc(IV)_{aq}$ was rapidly sorbed. Reduction of Tc(VII) to Tc(IV) occurred with Fe(II)-containing solid phases but not by aqueous Fe(II) species [12].

Lieser and Bauscher [13] observed wide variations in ^{99}Tc distribution coefficients for sediment-water experiments performed under aerobic and anaerobic conditions. By varying the redox potential, they observed a change in the K_d by about 3 orders of magnitude within a small range of Eh at 190 ± 30 mV for a pH of 7 ± 0.5. Chemical equilibrium modeling using EQ3/6 software has also shown the enhanced retardation of ^{99}Tc under reducing conditions in the saturated zone at Yucca Mountain [14]. To summarize, Tc can behave as either a non-sorbing species (like chloride) or a strongly sorbing species (like Am) – simply because of a modest change in redox conditions. The assumption that ^{99}Tc will always behave as a mobile species may therefore be too conservative.

Iodine-129

The fate and transport of ^{129}I in groundwater is also dictated by its chemical speciation. Aqueous iodine usually occurs as the highly mobile iodide anion (I^-). Under more oxidizing conditions, iodine will be present as the iodate anion (IO_3^-), which is more reactive than iodide and could be sorbed onto positively-charged sites locally existing in clays and organic matter [15-16]. Unlike other redox-sensitive radionuclides (such as ^{99}Tc), iodine sorption may *decrease* under reducing conditions when I^- is the predominant species. However, coexistence of several iodine species

(iodide, iodate, and organic iodine species) has been reported in various aqueous systems [17], which will tend to make the sorption behavior of iodine more difficult to predict.

Actinides

A large volume of literature exists on the geochemical behavior of actinides in the environment; topical review papers include Kim [18], Dozol and Hagemann [19], Silva and Nitsche [20], and Kersting and Reimus [21]. In general, the mobility of actinides in aqueous systems is dependent on (1) their thermodynamic properties, which determine solubility and speciation as a function of pH and redox potential, (2) the availability of inorganic and organic ligands to form soluble complexes, and (3) the composition and abundance of minerals and mineral colloids present in the system. The valence state of redox sensitive radionuclides (including U, Np and Pu) plays a major role in defining the geochemical reactions and migration behavior of these elements. Solubility-limited concentrations, complexation reactions, sorption onto minerals, and colloid formation all differ considerably as a function of oxidation state [22].

The chemistry of uranium in the environment is dominated by the difference in behavior of the U(IV) and U(VI) ions. The tetravalent form generally has low solubility whereas the hexavalent form is relatively soluble as the uranyl (UO_2^{2+}) ion and its complexes [23]. As shown in Figure 2a, the uranyl ion commonly forms soluble complexes with carbonate ligands at pH values typical of NTS groundwaters [24-25]. Even at relatively low oxidation potentials, uranyl species may dominate aqueous uranium speciation, although uraninite (UO_2) is the stable solid phase. Uranium is more readily sorbed onto minerals or organic matter when present as the positively charged uranyl species, and this step may precede reduction to less soluble U(IV) solids [26-29]. However, the strong affinity of carbonate ligands for uranyl in solution effectively competes with sorption, thereby limiting the sorption of uranyl carbonate complexes [23].

An important feature of neptunium chemistry in aqueous systems is the large stability range for Np(V) [30]. The pentavalent NpO_2^+ species is dominant at pH values <8 whereas Np(V) carbonate complexes tend to dominate at higher pH values [22] (Figure 2b). Since Np(V) solid phases are relatively soluble and Np(V) aqueous species do not easily sorb onto common minerals, Np(V) is relatively mobile in the environment. Under reducing conditions, Np(IV) is present as the low solubility $Np(OH)_4$ (aq) species at pH values >5 [22]. Np(IV) shows a strong tendency for sorption to mineral surfaces [30-31], which limits its mobility in aqueous systems.

The redox speciation of plutonium is affected by a number of competing variables, and Pu is observed to coexist in multiple valence states in natural waters [32] (Figure 2c). Pu(III) and Pu(IV) tend to be less stable than Pu(V) and Pu(VI) under oxidizing, near-neutral pH conditions, though Pu(IV) exhibits the strongest tendency to form ligand complexes [33]. The aqueous chemistry of plutonium is further complicated by the fact that Pu(IV) disproportionates to Pu(III) and Pu(VI), Pu(V) disproportionates to Pu(IV) and Pu(VI), and Pu(VI) is easily reduced [34-35]. Kersting and Reimus [21] showed that Pu(V) reduction to Pu(IV) is an important mechanism for Pu sorption to mineral surfaces.

Figure 3 summarizes the valence states for several radionuclides as a function of redox potentials, and the figure also includes the expected equilibrium redox potentials associated with the common electron-acceptor couples encountered in groundwater. In the laboratory experiments conducted during this study, the redox conditions were controlled by modifying the oxygen concentration in air, and by spiking the solutions with Fe^{2+} and S^{2-}.

Experimental methods

Materials

The extent of sorption of radionuclides is dependent on the physical and chemical properties of the radionuclide-aquifer-groundwater system. The lithologic (aquifer) materials used in this study included alluvium, welded/devitrified tuff, zeolitic tuff, and carbonate. All lithologic materials were crushed and sieved to a 75-500 μm size range [5]. The alluvium was collected from an exposed section of the U-1a.102 drift in the U-1a tunnel complex (at a depth of 295 m below the land surface) beneath Yucca Flat. The devitrified tuff sample was a Topopah Spring welded volcanic tuff collected from the Yucca Mountain tunnel (~300 m below ground surface). The original glassy matrix in this material has altered to fine-grained crystalline solids that include feldspar, quartz, cristobalite, and some smectite [37]. The zeolitic tuff sample was from drill core UE-7az (496 m below ground surface) within the tuff confining unit (TCU) of Yucca Flat. Zeolitic tuff is formed by the alteration of glassy vitric tuff near and below the water table [38], and is typically comprised of clinoptilolite (>60%), mordenite, opal, feldspar, and quartz. The carbonate rock was from drill core ER-6-1 (833 m below ground surface) within the lower carbonate aquifer (LCA) at Yucca Flat, and consists of massive dolomite with calcite veinlets.

A companion synthetic groundwater was used for each solid matrix. Synthetic LCA (Ca-Mg-HCO_3) and TCU (Na-K-HCO_3) waters were used in carbonate and zeolitic tuff sorption experiments, respectively. The solution compositions were based on measured concentrations of major ions in groundwaters sampled from the respective hydrostratigraphic units, except that sulfate, nitrate, and fluoride were omitted from the background solution because of their minimal role in radionuclide retardation processes. Synthetic J-13 water (Na-K-HCO_3 type) was used for the sorption of radionuclides onto alluvium and devitrified tuff. According to the thermodynamic database “thermo” in the Geochemist’s Workbench, a solution composed of J-13 water should be supersaturated with respect to a number of phases, including calcite [39]. To avoid potential

mineral precipitation issues, synthetic J-13 water was prepared using a recipe from Viani [39] that is predicted to be stable at 25 °C and atmospheric pCO_2.

Reagents

The radionuclides and surrogate species used in the batch-sorption experiments were chosen because they represent a significant fraction of the radiologic source term at the NTS, and are expected to show a wide range of radionuclide retardation behavior. Synthetic groundwaters were spiked with radionuclides and surrogate species at the appropriate amount to achieve the target concentration (Table 2). The target concentration was based on a combination of instrument detection limits, expected background concentrations, and solubility limits. Tables 2A, 2B, and 2C summarize the measured radionuclide composition used in each background solution. The stock solution for radionuclides (^{99}Tc, ^{237}Np, and ^{242}Pu) was stored in a HNO_3 matrix, a small amount of NH_4OH was added to adjust the sorption solution pH to that of background solution.

Chemical forms used in the initial solution were Sr^{2+}, Cs^{+}, I^{-}, $^{99}TcO_4^{-}$, and ReO_4^{-}. Valence states for the actinides were U(VI), $^{237}Np(V)$, and $^{242}Pu(IV)$; the predominant chemical forms are expected to be carbonate and/or hydroxide complexes for U, Np, and Pu. These are the valence states and chemical forms expected to occur in the oxidizing groundwaters at the NTS. Cs and Sr are not subject to changes in oxidation state and were included for comparison. ReO_4^{-} is sometimes used as the surrogate for TcO_4^{-} based on their similar crystal chemistry, electronic configuration, and thermodynamic data [40-42]. The Eh–pH diagrams for Tc and Re show that very similar Eh–pH fields are occupied by aqueous species (TcO_4^{-} and ReO_4^{-}) and by solids of Tc and Re. The main difference between Re and Tc is in their respective oxidation potentials; the reduction of Re is more difficult than that of Tc [43-44].

Radionuclides ^{242}Pu and ^{237}Np used in the batch sorption solutions were from existing stock in our laboratory. Standard Reference Materials, SRM 4288A for ^{99}Tc, SRM 4341 for ^{237}Np, and SRM 4334H for ^{242}Pu, obtained from the National Institute of Standards and Technology, were used to prepare the standard solution to calibrate the ICP-MS instrument for measuring the radionuclide concentrations in the batch-sorption samples.

Experimental procedure

The first batch test (Test A in Table 2) was carried out under atmospheric conditions. The test was conducted in accordance with ASTM method D4646 [45], except that a solution to solid ratio of 5:1 (one gram of air-dry solid to 5 mL of sorption solution) was employed instead of the 20:1 ratio specified in the ASTM method. All sorption treatments (solid and sorption solution) were run in triplicate. Blank (solid and background solution) and control (no solid; only sorption solution) treatments were run in duplicate.

A 0.7 m^3 glove box was used to modify and control the atmospheric composition for the other batch sorption experiments (Tests B-E). Either high purity Ar or a mixture of 99% Ar and 1% CO_2 was used to control the atmosphere composition inside the glove box. Tests B and C were conducted under a gas composition of about 1 and 0.1% O_2, controlled by maintaining the flow rate (pressure) of the pure Ar gas. Tests D and E were all conducted at 0.1% O_2 level, with test tubes further spiked with a reductant ($FeCl_2$ for Test D or Na_2S for Test E) (Table 2). Two gas sensors were placed inside the glove box to monitor air composition. The oxygen sensor (Pro O_2 analyzer, Nuvair Gas Analyzers, Oxnard, CA) has a detection limit of 0.1% O_2. A CO_2/temperature sensor (Model 7001, Telaire, Goleta, CA) was used to monitor the concomitant decrease of CO_2 with O_2 and to confirm the decreased O_2 level inside the glove box. The CO_2

sensor (working range of ~400 to 1 ppm) is more sensitive than the O_2 sensor (working range of 21 to 0.1%). The experimental temperature was 22.9±0.5 ºC.

During the sorption experiments conducted inside the glove box, 15-ml sized centrifuge tubes were uncovered to permit gas exchange and placed on a shaker (Maxi-Mix III type 65800, Thermolyne, Dubuque, IA) at a shaker speed of 1,000 rpm. Batch tests were started when the O_2 level inside the glove box reached steady-state levels, usually after 2-4 hours' flushing. Then after 48 hours, batch sorption tests were stopped and the sample was filtered with a 0.2 µm PTFE membrane syringe filter (Acrodisc CR 13 mm, Pall Life Sciences, East Hills, NY). The potential sorption kinetics of radionuclides and the limited mixing during sorption experiments was not evaluated, as this study was intended to compare the effects of redox conditions on sorption under otherwise similar experimental conditions.

An aliquot of filtrate (0.5 mL) was pipetted into 3.5 mL 2% HNO_3 solution for subsequent ICP-MS (Thermo Electron Model X7, Thermo Fisher Scientific, Inc, Waltham, MA) analysis of all elements of interest; 5 ng/L of ^{6}Li, ^{45}Sc, ^{115}In, and ^{209}Bi were included as internal standards. The redox potential, relative to the standard hydrogen electrode, was measured using platinum as a sensing electrode and silver–silver chloride as a reference electrode (Thermo Orion Eh combination electrode, model 9678BN, Thermo Fisher Scientific, Inc, Waltham, MA) filled with saturated potassium chloride. Standard Zobell's solution (a solution of potassium ferric–ferrocyanide of known Eh) was used to verify the working operation of the measurement system [46]. Measurement of pH for the filtrate was conducted using an Oakton meter (Eutech Instruments, Singapore) and glass pH electrode system (Orion Ross combination pH electrode, model 81-02) calibrated to three pH buffer standards (pH 4, 7, and 10). Dissolved oxygen in the

filtrate was evaluated with a SympHony SB50D (Thermo Orion) with a detection limit of 0.1 mg/L. All these measurements were performed inside the glove box under the desired O_2 level.

Evaluation of redox conditions

The principal redox couples in the subsurface are O_2/H_2O, NO_3^-/N_2, Mn(IV, III)/Mn(II), Fe(III)/Fe(II), SO_4^{2-}/H_2S, and CO_2/CH_4, which form a redox ladder from the most oxidizing O_2/H_2O to the reducing CO_2/CH_4 couples. The theoretical (thermodynamically calculated) Eh values at pH 7 are 816, -182, and -215 mV for the O_2/H_2O, Fe(III)/Fe(II), and SO_4^{2-}/H_2S redox couples employed in this study. However, various authors caution the use of Eh in quantifying redox condition [47-48]. The difficulty in interpreting redox from Eh measurements results from using an equilibrium approach to describe a highly dynamic system [49]. Eh is a simple measure, but it gives at best only qualitative assessment of water redox conditions because the Pt electrode may not respond to many important redox couples.

As summarized in Tanji et al. [48], many researchers have found a Pt electrode may not reflect changes in some species involved in redox reactions, such as partial pressure of O_2, and neither Mn/Fe oxides nor nitrate had the expected quantitative effect on the Pt electrode measurement. Methane, bicarbonate, nitrogen gas, nitrate and sulfate cannot readily take up or give off electrons at the surface of Pt electrode. Redox electrodes do not respond quantitatively to the redox couples in solution because they are not at redox equilibrium with the platinum electrode. Thus, a wide range of Eh has been observed for the same redox couple and, as a result, several redox reactions may be relevant within the same Eh range [50]. The measured Eh usually reflects “non-equilibrium” potentials and can only be qualitatively interpreted. Supplementary measurements of redox couple concentrations should be made in addition to Eh measurements to better evaluate redox conditions.

In this work, Eh values measured with a platinum electrode did not appear to reflect the Eh difference between the SO_4^{2-}/H_2S and Fe(III)/Fe(II) redox couples; the Eh values in Test E were all consistently higher than in Test D (see discussion of Table 3, below). In addition to the Eh measurements, sulfate production in the sulfate/sulfide redox couple was monitored. In Test E where 24 mg/L (0.3 mM) Na_2S was spiked into the sorption solution, about 2 mg/L sulfate (SO_4^{2-}) was produced. According to the reaction:

$$S^{2-} + 4H_2O = SO_4^{2-} + 8H^+ + 8\ e^- \quad (1)$$

this amount was equivalent to 0.67 mg/L sulfide (S^{2-}) being oxidized and suggested that sufficient sulfide remained in solution to influence redox conditions.

Results and discussion

Utility of glove box to control redox conditions

We first evaluated the approach of producing and maintaining different redox conditions in the radionuclide-aquifer-groundwater system by controlling the air composition inside a glove box. This was accomplished by replacing the ambient air with 1% CO_2 in Ar. The change of oxygen content as a function of flow rate was controlled by adjusting incoming gas pressure; a steady-state level of O_2 inside the glove box was reached at about 2 hours under 10 psi and at 4 hours under 1 psi. Figure 4 shows the change of solution Eh in response to the flushing-out process of air inside a glove box. The Eh was periodically measured in background solutions, and all three background solutions exhibited a similar trend (i.e., similar behavior in redox buffering) (Figure 4a). Figure 4b shows the effect of gas-water interface area and the redox buffering capacity of the crushed rock (devitrified tuff, in this case). As expected, J-13 water placed in a centrifuge tube (1.8 cm^2 gas-water interface) responded, in terms of solution Eh, more slowly than that in a beaker with a gas-water interface area 9 times larger. The presence of solids (devitrified tuff,

which provides buffering capacity) contributed to the maintenance of a higher solution Eh. Limited measurements of solution pH in J-13 water showed a slight decrease from 7.91 at 20.9% O_2 to 7.67 at 10.3% O_2, while pH value for J-13 and devitrified tuff at the same O_2 levels decreased from 8.0 to 7.2.

The test demonstrates the feasibility of achieving a range of more than 200 mV in Eh under these experimental condition; further reduction can be obtained by applying a reductant ($FeCl_2$ or Na_2S) in the sorption system. For Tests D and E, a small amount of $FeCl_2$ or Na_2S was added into the sorption solution, and pH was adjusted (with either NH_4OH and/or HNO_3) to be the same as the value before the spiking of the reductant.

Sorption in radionuclide-aquifer-groundwater systems

Figures 5-9 present the measured K_ds (average ± standard deviation for triplicates) of each radionuclide onto four different aquifers under six different redox conditions. *The measured values were not necessarily the sorption coefficients at equilibration; the objective of these experiments was to study the relative effect of redox condition on radionuclide sorption under otherwise similar conditions.* In addition, the term sorption is loosely used in this work to describe the concentration decrease in the solution phase of radionuclides, which could include sorption onto the solid as well as surface precipitation.

By modifying the air composition and adding a reductant, we achieved an Eh range of nearly 400 mV from Tests A to E measured at the end of 48 hours experimental duration (Table 3). As expected, for elements that were insensitive to redox conditions (i.e., Sr and Cs), K_d values generally did not vary as a function of Eh for all four radionuclide-aquifer-groundwater systems (Figure 5); observed small differences for carbonate and zeolitic tuff were probably related to the sample and analytical variability. Compared to the change in Eh, values of pH among all treatments were relatively stable (Table 4).

As solutions become more reducing from Tests A to E, the Tc K_d tended to increase. This was especially evident for devitrified tuff (Figure 6), but was also noticeable for Test E in alluvium and zeolitic tuff. Re sorption also increased under more reducing conditions in devitrified tuff, alluvium, and zeolitic tuff, but the extent of increase was much smaller. This was consistent with the greater stability of oxidized Re compared to Tc (discussed in-*Reagents* section). As reported by Lieser and Bauscher [13], if TcO_4^- is reduced by Fe(II) according to the reactions

$$3Fe^{2+} + TcO_4^- + 8H_2O = 3Fe(OH)_3 + TcO(OH)_2 + 5H^+, \quad (2)$$

hydrolytic adsorption of $TcO(OH)_2$ on iron (III) hydroxide or coprecipitation with Fe(III) by formation of hydroxo complexes containing Fe–O–Tc bonds can be expected. When H_2S or S_2^- ions are present and the solubility product of the sparingly soluble Tc_2S_7 is exceeded, precipitation or coprecipitation of Tc_2S_7 may also occur.

The increasing Tc K_d value as a function of Eh was particularly significant for devitrified tuff; the Tc K_d value in Test E was 300 times higher than in Test A. It is not clear why the Eh decrease to a moderately reducing condition only has an effect on ^{99}Tc sorption/precipitation in devitrified tuff. It is likely that a combination of factors contribute to the observed effect, these factors including changes in the sorbate (redox speciation), the sorbent (surface properties), and the water chemistry (such as pH and Fe^{2+}/S^{2-} concentrations). It is possible that the devitrified tuff has a trace amount of reducing mineral that is not measurable by X-ray diffraction. The Fe_2O_3 content (wt %) measured by X-ray fluorescence was reported to be 0.96±0.092 for devitrified and 0.84 for zeolitic tuff, respectively [37]. The four aquifer materials had different aqueous iron concentrations after contact with background water, and also exhibited different response to added Fe^{2+} (Table 5). Both alluvium and devitrified tuff released some iron, but the alluvium seemed to be able to sorb added Fe^{2+} very effectively. Carbonate rock appeared to have effectively sorbed the added Fe^{2+} in Test D. Zeolitic tuff could release significant amounts of

iron, and the amount released decreases from Tests A to C with an associated decrease in Eh value.

For the interaction of Tc with alluvium, there was essentially no sorption in Tests A to D (Figure 6). The measurable, though small, sorption of Tc in Test E for alluvium and zeolitic tuff suggested that Tc will be slightly retarded if the radionuclide encounters a reducing zone along its flowpath.

Some level of iodine (applied as iodide) sorption was observed in nearly all samples (K_d = 0 – 0.99 mL/g). However, this sorption did not appear to be correlated with redox (Figure 7), therefore, some iodine retardation will help limit its transport in the subsurface at the NTS at any redox condition. Furthermore, the range of K_d is substantially lower (and narrower) than the range proposed in Table 1, which is from the literature values confounded by iodine speciation (discussed in *Background*).

Sorption of Np in devitrified tuff also increased significantly with decreasing Eh; the Np K_d value in Test E was 200 times higher than in Test A. It appears that a substantial quantity of Np(V) was reduced to Np(IV), leading to a strong retention similar to Pu(IV). This suggests that Np may be substantially retarded in mildly reducing groundwater conditions, contrary to most Np transport predictions which assume that Np remains in the +5 oxidation state. Conversely, there was little change in Np sorption on alluvium and carbonate aquifer materials as a function of redox condition, which implies strong Np sorption to minerals in these two materials (e.g., calcite). Similar to what we obtained for Test A under atmospheric condition, low K_d values have been reported for Np in tuff [4], while nearly two orders of magnitude larger K_d values were reported in carbonate [51]; Figure 8 shows a similar trend. Figure 10 presents the experimental Eh-pH ranges studied in this work overlaid on Np stability field plots for Np in LCA water. The

likely Np species encountered in J-13 water would include $NpO_2CO_3^-$, NpO_2^+, and $Np(OH)_4$ (Figure 2b). The reduced $Np(OH)_4$ species is likely to sorb (or precipitate) much more strongly than the oxidized species, which is consistent with our observations of an increasing trend of Np K_d with decreasing Eh for devitrified tuff in J-13 water (Figure 2b). For Np sorption in carbonate (Figure 10), $NpO_2CO_3^-$ and NpO_2^+ species might have as strong an interaction with carbonate minerals as $Np(OH)_4$ species, which would minimize the effect of Eh (Figure 8).

Overall, uranium K_d values in Tests B to E for alluvium, devitrified tuff, and zeolitic tuff were larger than in Test A, which was conducted under atmospheric conditions (Figure 9a). Uranium sorption to carbonate in Tests D and E were anomalous (negative K_d value of 2.6-3.9 mL/g that was too large to be considered experimental error). These samples also had anomalously low initial concentrations (Table 2c). The reasons for the anomalous behavior of uranium in the carbonate system are unknown. The low initial concentration for Tests C and D was also observed for iodine and Pu (Table 2c).

Using 1 mM sulfide, Beyenal et al. [52] reported the reduction and total removal of about 53,000 µg/L (140 µM) U(VI) from solution. The U(VI) was found to be precipitated as U(IV)-uraninite. We used ~0.33 mM sulfide (24 ppm Na_2S) and an initial U(VI) concentration of ~1,000 µg/L. The highest K_d measured under these conditions was 268 mL/g (98% removal, devitrified tuff); the lowest was 8 mL/g (60% removal, zeolitic tuff). Hua et al. [53] suggested the reaction stoichiometry of U(VI) reduction by hydrogen sulfide could be best described by

$$HS^- + UO_2^{2+} = UO_2 + S^0 + H^+. \quad (3)$$

The kinetics of U(VI) reduction was found to be largely controlled by the total carbonate concentration and pH. They further concluded that uranium-hydroxyl species, not the dominant U-carbonate species, were the ones being reduced by sulfide. Our experiments suggest that a

combination of water chemistry and rock mineralogy will affect the efficiency of sulfide-promoted U(VI) reduction.

Overall, Pu sorption was not significantly affected by the decreasing redox conditions achieved in this study (Figure 9b). This was especially evident for alluvium and zeolitic tuff samples. The predominant Pu species at all redox conditions achieved in our experiments was the sparingly-soluble and strongly sorbing $Pu(OH)_4$ (Figure 2c). At low pH (<7) and highly reducing conditions, Pu may exist as Pu(III). However, this species is also a very strong sorber. Overall, Pu sorption onto NTS aquifer rocks is much less affected by redox than other redox-sensitive radionuclides.

Variable redox conditions in the subsurface

Considering the importance of reducing groundwaters in retarding redox-sensitive radionuclide transport, more efforts are needed to elucidate the presence of variable redox conditions in the subsurface. Using a flow-through cell to sample well-pumped groundwater and perform high-quality measurements of geochemical parameters (e.g., Eh, dissolved oxygen, pH), as well as several redox couples (Fe^{2+}/Fe^{3+}, Mn^{2+}/Mn^{4+}, $NO_2^-/NO_3^-/NH_4^+$) will help reliably assess the redox condition observed in the groundwater wells.

We performed iodine speciation analysis for a total of 43 NTS groundwater samples, and found that 79% of the samples had iodide concentrations of less than 50% of the total iodine, which indicated that the groundwater in the deep NTS aquifer exhibited variable redox conditions. Variations in redox conditions have also been documented in other deep aquifer systems. For example, variations in the concentrations of dissolved Fe species, H_2S, DO, and Eh were used to identify changes in redox conditions along a flow path in the Carrizo Sand aquifer of Texas (with a lateral sampling distance of 66 km and well depth ranging 122–1,420 m) and the Upper

Floridan carbonate aquifer of Florida (a sampling distance of 144 km and well depth 61–155 m) [54-55]. In both aquifers, oxic to suboxic conditions were observed near the recharge area, while mildly reducing groundwaters existed further down the flow path.

Localized mildly-reducing conditions with Fe(II), sulfate and sulfide in the water, and more strongly-reducing conditions with the presence of methane have often been explained by the presence of microniches inside or in the vicinity of organic matter being oxidized [56]. Two types of microniches were suggested by Jakobsen [56] on the grain scale, particles of organic matter and intragranular microniches such as grain cracks containing organic matter. It was recently shown in Darling [57] that methane in low concentrations was present in many aquifer systems.

Some experimental evidence from the Nevada Test Site has pointed to the importance of changes in redox conditions during the transport of redox-sensitive radionuclides. For example, at Cheshire (a nuclear test at the NTS), ^{99}Tc concentrations were observed to drop precipitously in groundwater samples having high concentrations of iron-rich colloidal particles (possibly iron oxyhydroxides), while ^{36}Cl was not affected [58]. No explanation was offered, though it seems probable that the reduction of Tc(VII) to Tc(IV) and formation of insoluble Tc precipitates were the cause, when ferrous iron was present to moderate the reduction.

Conclusions

This work describes the effect of reducing groundwater on the retardation of redox-sensitive radionuclides in the NTS. Based on our review of literature and experimental results, we have the following conclusions:

- Laboratory batch-sorption experiments showed markedly greater retardation for some radionuclides (especially ^{99}Tc and ^{237}Np in devitrified tuff) under reducing conditions. Retardation of radionuclides as a function of redox condition is particularly important for ^{99}Tc, which would be highly mobile under oxidizing conditions. The ^{99}Tc K_d in devitrified tuff correlated with redox, increasing from 1.22 to 378 mL/g from oxidizing to mildly reducing. Under oxidizing conditions, measured ^{99}Tc K_d values were 0.12–0.81 in carbonate rock, 0.045–0.61 mL/g in zeolitic tuff, and ~0 in alluvium.

- Under the experimental conditions, values for K_d of iodine are marginally correlated with redox; K_ds were 0.33–0.99, 0.43–0.90, 0–0.72 and 0–0.79 mL/g for alluvium, devitrified tuff, carbonate, and zeolitic tuff. Importantly, a non-zero K_d was observed in all samples, suggesting that ^{129}I transport will be retarded. Including the measurable K_d for ^{129}I iodine would result in less conservative and more realistic radionuclide transport predictions.

- The Np K_d strongly correlated with redox condition in devitrified tuff, with an increase from 4.6 to 930 mL/g. The probable reduction of Np(V) to Np(IV), and comparable K_d to Pu(IV), under mildly reducing condition has not been widely reported in the literature. Overall, sorption of U for alluvium, devitrified tuff, and zeolitic tuff under atmospheric conditions was smaller than the glove-box tests. Sorption of Pu was not affected by the decreasing redox conditions achieved in this study, as the predominant Pu species in all conditions was expected to be low-soluble and strongly sorptive $Pu(OH)_4$.

Probable presence of reducing groundwater zones in the subsurface could potentially contribute to the retardation of some redox-sensitive radionuclides. Understanding of redox conditions on the transport of redox-sensitive radionuclides garnered from this study on the NTS is very important to the process understanding and remediation strategy in other contaminated sites.

Acknowledgments

Funding for this investigation was provided by the Environment Restoration Division's Underground Test Area Project at the U.S. Department of Energy, National Nuclear Security Administration, Nevada Site Office. This work was performed under the auspices of the U.S. Department of Energy by Lawrence Livermore National Laboratory (LLNL) under Contract DE-AC52-07NA27344.

References

1. Ahearne JF: **Radioactive waste: The size of the problem**. *Physics Today* 1997, **50(6)**: 24–29.

2. Ewing RC: 2004. **Environmental impact of the nuclear fuel cycle**. In Energy, Waste and the Environment: A Geochemical Perspective. Edited by Gieré R. Stille P. Geological Society Special Publication 236, The Geological Society, London, 2004, 7–23.

3. Smith DK, Finnegan DL, Bowen, SM: **An inventory of long-lived radionuclides residual from underground nuclear testing at the Nevada test site, 1951-1992**. *Journal of Environmental Radioactivity* 2003, **67**: 35–51.

4. Stoller-Navarro Joint Venture (SNJV): Phase II Contaminant Transport Parameters for the Groundwater Flow and Contaminant Transport Model of Corrective Action Unit 98: Frenchman Flat, Nye County, Nevada. Las Vegas, NV: S-N/99205-043, 2005, 458 p. http://www.osti.gov/energycitations/product.biblio.jsp?osti_id=875996 (checked on 5/8/2008).

5. Triay IR, Meijer A, Conca JL, Kung KS, Rundberg RS, Strietelmeier BA, Tait CD: Summary and synthesis report on radionuclide retardation for the Yucca Mountain Site Characterization Project. Los Alamos National Laboratory, Los Alamos, NM**:** Milestone 3784M, 1997.

6. Zavarin M., Carle SF, Maxwell RM: Upscaling radionuclide retardation – Linking the surface complexation and ion exchange mechanistic approach to a linear Kd approach. Lawrence Livermore National Laboratory, Livermore, CA: UCRL-TR-204713, 2004,

164 p. http://www.osti.gov/energycitations/product.biblio.jsp?osti_id=15014299 (checked on 5/8/2008).

7. Eriksen TE, Ndalamba P, Bruno J, Caceci M: **The solubility of $TcO_2 \cdot nH_2O$ in neutral to alkaline solutions under constant pCO_2**. *Radiochimica Acta* 1992, **58/59**: 67–70.

8. Bondietti EA, Francis CW: **Geologic migration potentials of Tc-99 and Np-237**. *Science* 1979, **203**: 1337–1340.

9. BSC (Bechtel SAIC Company); Site-Scale Saturated Zone Transport. Appendix F: Redox Measurements in Saturated Zone Waters. NDL-NBS-HS-000010, Rev. 02. Las Vegas, Nevada: Bechtel SAIC Company, 2004. 297–312. http://www.osti.gov/energycitations/purl.cover.jsp?purl=/886569-1Bv4Ne/ (checked on 5/8/2008).

10. Cui D, Eriksen TE. **Reduction of pertechnetate in solution by heterogeneous electron transfer from Fe(II)-containing geological material**. *Environmental Science and Technology* 1996**, 30**: 2263–2269.

11. Cui D, Eriksen TE: **Reactive transport of Sr, Cs and Tc through a column packed with fracture-filling material**. *Radiochimica Acta* 1998, **82**: 287–292.

12. Cui D, Eriksen TE: **Reduction of pertechnetate by ferrous iron in solution: Influence of sorbed and precipitated Fe(II)**. *Environmental Science and Technology* 1996, **30**: 2259–2262.

13. Lieser KH, Bauscher CH: **Technetium in the hydrosphere and in the geosphere. I. Chemistry of technetium and iron in natural waters and influence of the redox potential on the sorption of technetium**. *Radiochimica Acta* 1987, **42**: 205–213.

14. Arnold BW, Meijer A, Kalinina E, Robinson BA, Kelkar S, Jove-Colon C, Kuzio SP, James S, Zhu M: Impacts of reducing conditions in the saturated zone at Yucca Mountain. Proceedings of the 11th International High- Level Radioactive Waste Management Conference (IHLRWM), Las Vegas, NV, 2006, 345–352.

15. Couture RA, Seitz MG: **Sorption of anions of iodine by iron oxides and kaolinite**. *Nuclear Chemistry and Waste Management* 1983**, 4**: 301–306.

16. Sheppard M, Thibault DH: **Chemical behavior of iodine in organic and mineral soils**. *Applied Geochemistry* 1992**, 7**: 265–272.

17. Hu QH, Zhao P, Moran JE, Seaman JC: **Sorption and transport of iodine species in sediments from the Savannah River and Hanford Sites**. *Journal of Contaminant Hydrology* 2005, **78(3)**: 185–205.

18. Kim JI: *Chemical behaviour of transuranic elements in natural aquatic systems*. In Handbook on the Physics and Chemistry of the Actinides, edited by Freeman AJ, Keller C, Elsevier, Amsterdam, 1986**, 4**: 413–455.

19. Dozol M, Hagemann R: **Radionuclide migration in groundwaters: Review of the behaviour of actinides**. *Pure and Applied Chemistry* 1993, **65**: 1081–1102.

20. Silva RJ, Nitsche H: **Actinide environmental chemistry**. *Radiochimica Acta* 1995, **70/71**: 377–396.

21. Kersting AB, Reimus PW: Colloid-Facilitated Transport of Low-Solubility Radionuclides: A Field, Experimental, and Modeling Investigation. Lawrence Livermore National Laboratory Report, Livermore, CA: UCRL-ID-149688, 2003, 285 p. http://www.osti.gov/energycitations/product.biblio.jsp?osti_id=15006520 (checked on 5/8/2008).

22. Kaszuba JP, Runde WH: **The aqueous geochemistry of neptunium: Dynamic control of soluble concentrations with applications to nuclear waste disposal**. *Environmental Science and Technology* 1999, **33**: 4427–4433.

23. Murphy WM, Shock EL: *Environmental aqueous geochemistry of actinides*. In Uranium: Mineralogy, Geochemistry and the Environment. Reviews in Mineralogy, edited by Burns PC, Finch R., Mineralogical Society of America, Washington, D.C., 1999, v. 38, 221–253.

24. Langmuir D: **Uranium solution-mineral equilibria at low temperatures with applications to sedimentary ore deposits**. *Geochimica et Cosmochimica Acta* 1978, **42**: 547–569.

25. Pabalan RT, Turner DR: **Uranium(6+) sorption on montmorillonite: Experimental and surface complexation modeling study**. *Aquatic Geochemistry* 1997, **2**: 203–226.

26. Zielinski RA, Meier A: **The association of uranium with organic matter in Holocene peat: An experimental leaching study**. *Aquatic Geochemistry* 1988, **3**: 631–643.

27. Carroll SA, Bruno J, Petit J-C, Dran J-C: **Interactions of U(VI), Nd, and Th(IV) at the calcite-solution interface**. *Radiochimica Acta* 1992, **58/59**: 245–252.

28. Barnes CE, Cochran JK: **Uranium geochemistry in estuarine sediments: Controls on removal and release processes**. *Geochimica et Cosmochimica Acta* 1993, **57**: 555–569.

29. Wersin P, Hochella MF Jr, Persson P, Redden G, Leckie JO, Harris DW: **Interaction between aqueous uranium (VI) and sulfide minerals: Spectroscopic evidence for sorption and reduction**. *Geochimica et Cosmochimica Acta* 1994, **58**: 2829-2843.

30. Lieser KH, Mühlenweg U: **Neptunium in the hydrosphere and in the geosphere.1. Chemistry of neptunium in the hydrosphere and sorption of neptunium from groundwaters on sediments under aerobic and anaerobic conditions**. *Radiochimica Acta* 1988, **43(1)**: 27–35.

31. Nakata K, Nagasaki S, Tanaka S, Sakamoto Y, Tanaka T, Ogawa H: **Sorption and reduction of neptunium (V) on the surface of iron oxides**. *Radiochimica Acta* 2002, **90**: 665–669.

32. Nitsche H, Silva RJ: **Investigation of the carbonate complexation of Pu(IV) in aqueous solution**. *Radiochimica Acta* 1996, **72**: 65–72.

33. Choppin GR, Bond AH, Hromadka PM: **Redox speciation of plutonium**. *Journal of Radioanalytical and Nuclear Chemistry* 1997, **219(2)**: 203–210.

34. Clark DL, Hobart DE, Neu MP: **Actinide carbonate complexes and their importance in actinide environmental chemistry**. *Chemical Review* 1995, **95**: 25–48.

35. Silver GL: **Proportional equations in plutonium chemistry**. *Journal of Radioanalytical and Nuclear Chemistry* 2000, **245(2)**: 229–232.

36. Banaszak JE, Rittmann BE, Reed DT: **Subsurface interactions of actinide species and microorganisms: Implications for the bioremediation of actinide-organic mixtures**. *Journal of Radioanalytical and Nuclear Chemistry* 1999, **241(2)**: 385–435.

37. Vaniman DT, Chipera SJ, Bish DL, Carey JW, Levy SS: **Quantification of unsaturated-zone alteration and cation exchange in zeolitized tuffs at Yucca Mountain, Nevada, USA**. *Geochimica et Cosmochimica Acta* 2001 **65(20)**: 3409–3433.

38. Bish DL, Vaniman DT, Chipera SJ, Carey JW: **The distribution of zeolites and their effects on the performance of a nuclear waste repository at Yucca Mountain, Nevada, USA**. *American Mineralogist* 2003, **88(11-12)**: 1889–1902.

39. Viani B: Formulation of recipes for synthetic J-13 groundwater that are predicted to be stable at 25 °C and atmospheric pCO_2. Internal report, Lawrence Livermore National Laboratory, Livermore, CA, 2002.

40. Brookins DG: **Rhenium as analog for fissiogenic technetium: Eh-pH diagram (25 ^{o}C, 1 bar) constraints**. *Applied Geochemistry* 1986, **1**: 513–517.

41. Harvey BR, Williams KJ, Lovett MB, Ibbett RD: **Determination of technetium-99 in environmental material with rhenium as a yield monitor**. *Journal of Radioanalytical and Nuclear Chemistry* 1992, **158(2)**: 417–436.

42. Wharton M J, Atkins B, Charnock JM, Livens FR, Pattrick RAD, Collins D: **An X-ray absorption spectroscopy study of the coprecipitation of Tc and Re with mackinawite (FeS)**. *Applied Geochemistry* 2000, **15**:347–354.

43. Richter RC, Koirtyohann SR, Jurisson SS: **Determination of technetium-99 in aqueous solutions by inductively coupled plasma mass spectrometry: Effects of chemical form and memory.** *Journal of Analytical and Atomic Spectrometry* 1997, **12**: 557–562.

44. Mas JL, Tagami K, Uchida S: **Method for the detection of Tc in seaweed samples coupling the use of Re as a chemical tracer and isotope dilution inductively coupled plasma mass spectrometry**. *Analytica Chimica Acta* 2004, **509(1)**: 83–88.

45. ASTM: Standard test method for 24-hour batch-type measurement of contaminant sorption by soils and sediments (D4646-87). In 1998 Annual Book of ASTM Standards. American Society for Testing and Materials, Philadelphia, PA., 1998, 44–47.

46. Nordstrom DK: **Thermochemical redox rquilibria of Zobells solution**. *Geochimica et Cosmochimica Acta* 1977, **41(12)**: 1835–1841.

47. Lindberg RD, Runnells DD: **Groundwater redox reactions: An analysis of equilibrium state applied to Eh measurements and geochemical modeling**. *Science* 1984, **225**: 925-927.

48. Tanji KK, Gao S, Scardaci SC, Chow AT: **Characterizing redox status of paddy soils with incorporated rice straw**. *Geoderma* 2003, **114(3-4)**: 333–353.

49. Bartlett RJ: Characterizing soil redox behavior. In Soil Physical Chemistry, edited by Sparks DL, Boca Raton, FL, CRC Press, 1999, 371–397.

50. Lovley DR, Goodwin S: **Hydrogen concentrations as an indicator of the predominant terminal electron-accepting reactions in aquatic sediments**. *Geochim. Cosmochim. Acta* 1988, **52**: 2993–3003.

51. Stout DL, Carroll SA: A literature review of actinide-carbonate mineral interaction. Sandia National Laboratories, Albuquerque, NM**:** SAND92-7328, 1992.

52. Beyenal H, Sani RK, Peyton BM, Dohnalkova AC, Amonette JE, Lewandowski Z: **Uranium immobilization by sulfate-reducing biofilms.** *Environmental Science and Technology* 2004, **38(7)**: 2067–2074.

53. Hua B, Xu HF, Terry J, Deng BL: **Kinetics of uranium(VI) reduction by hydrogen sulfide in anoxic aqueous systems**. *Environmental Science and Technology* 2006, **40(15)**: 4666–4671.

54. Haque S, Johannesson KH: **Arsenic concentrations and speciation along a groundwater flow path: The Carrizo Sand aquifer, Texas, USA**. *Chemical Geology* 2006, **228(1-3)**: 57–71.

55. Haque S, Johannesson KH: **Concentrations and speciation of arsenic along a groundwater flow-path in the Upper Floridan aquifer, Florida, USA**. *Environmental Geology* 2006, **50(2)**: 219–228.

56. Jakobsen R: **Redox microniches in groundwater: A model study on the geometric and kinetic conditions required for concomitant Fe oxide reduction, sulfate reduction, and methanogenesis**. Water Resources Research 2007, **43**, W12S12, doi: 10.1019/2006WR005663.

57. Darling WG: **The hydrogeochemistry of methane: Evidence from English groundwaters**. Chemical Geology 2006, **229**: 293–312.

58. Buddemeier RW, Finkel RC, Marsh KV, Ruggieri MR, Rego JH, Silva RJ: **Hydrology and radionuclide migration at the Nevada Test Site**. *Radiochimica Acta* 1991, **52/53**: 275–282.

Table 1: Radionuclide sorption on different rock (compiled from SNJV, 2005)

Element	Sample type	Number of Samples	Distribution Coefficients (mL/g)			
			Minimum	Maximum	Mean	Standard Deviation
Strontium	Alluvium	73	1	781	470	197
	Carbonate rock		5	16		
	Devitrified tuff	154	9	1,200	101	141
	Vitric tuff	30	23	220	148	62
	Zeolitic tuff	83	1,200	246,085	39,277	54,882
Technetium	Alluvium	17	0	12	2.16	3.48
	All tuffs		0	0		
Iodine	Alluvium	14	0	24.5	5.74	4.03
	All tuffs		0	0		
Cesium	Alluvium	56	1,720	33,200	5,884	5,153
	Carbonate rock		4	101		
	Devitrified tuff	159	10	3,800	645	656
	Vitric tuff	30	109	1,061	646	317
	Zeolitic tuff	86	2,700	72,000	16,747	13,710
Uranium	Alluvium	48	0.9	60	6.36	5.04
	Carbonate rock		0	132		
	Devitrified tuff	75	0	15	2.51	2.29
	Vitric tuff	59	0	12	1.89	1.7
	Zeolitic tuff	176	0	9,423	45	423
Neptunium	Alluvium	30	1.83	22	8.57	5.08
	Carbonate rock		<100	5,000		
	Devitrified tuff	421	0	2,353	19	166
	Vitric tuff	400	0	526	3.17	29
	Zeolitic tuff	430	0	22	3	2
Plutonium	Alluvium	24	230	21,000	4,091	4,448
	Carbonate rock		100	10,000		
	Devitrified tuff	118	6	1,900	125	168
	Vitric tuff	71	23	1,810	516	472
	Zeolitic tuff	110	19	2,000	260	242
Americium	Alluvium	24	3,200	1,400,000	174,469	214,582
	Carbonate rock		150	300,000		
	Devitrified tuff	35	79	12,000	1,845	1,834
	Vitric tuff	8	860	2,050	1,354	398
	Zeolitic tuff	25	470	33,000	5,204	7,757

Table 2A. Measured initial radionuclide concentrations (µg/L) in synthetic J-13 water

Test ID	Test Condition	Sr	Tc-99	I	Cs	Sm	Re	Np-237	U-238	Pu-242
A	Atmospheric	3,648±117 (4.16×10^{-5}) [a]	9.88 (9.99×10^{-8})	12,764±1137 (1.01×10^{-4})	1,112±38.5 (8.37×10^{-6})	14.6±1.55 (9.71×10^{-8})	159±5.09 (8.54×10^{-7})	199±5.66 (8.39×10^{-7})	1,192±36.2 (5.01×10^{-6})	0.0785±0.004 (3.24×10^{-10})
B	1% O_2	4,695±9.62	12.7±0.06	19,116±62.2	1,469±0.57	49.5±2.81	209±1.36	261±1.19	1,118±34.5	0.113±0.0001
C	0.1% O_2	4,598±11.3	12.4±0.00	18,616±679	1,439±2.26	41.0±36.1	204±0.40	258±0.06	1,518±11.3	0.111±0.017
D	11 ppm $FeCl_2$	3,190±162	8.91±0.29	2,071±481	993±40.7	30.0±38.0	151±4.53	148±6.62	393±477	0.032±0.036
E	24 ppm Na_2S	3,134±50.9	8.63±0.12	1,090±0.00	986±44.1	9.82±12.6	159±19.1	162±21.0	656±268	0.030±0.023

Table 2B. Measured initial radionuclide concentrations (µg/L) in synthetic LCA water

Test ID	Test Condition	Sr	Tc-99	I	Cs	Sm	Re	Np-237	U-238	Pu-242
A	Atmospheric	3,630±246	9.56±0.61	11,900±990	1,109±78.6	13.6±0.97	159±11.0	200±1.48	1,202±91.6	0.100±0.008
B	1% O_2	4,724±76.4	12.4±0.27	18,516±84.8	1,473±25.5	30.4±6.41	206±4.41	262±3.56	1,587±25.5	0.136±0.001
C	0.1% O_2	4,629±2.26	12.3±0.00	19,276±119	1,437±9.05	43.3±1.02	204±0.45	260±0.11	1,556±2.83	0.133±0.0002
D	11 ppm $FeCl_2$	3,656±522	9.72±1.39	1,968±87.7	1,099±158	3.83±4.62	162±23.1	139±21.0	62.1±81.0	0.008±0.008
E	24 ppm Na_2S	3,182±83.2	8.53±0.19	846±7.35	966	4.74±2.85	144±4.36	144±5.32	207±52.1	0.011±0.006

Table 2C. Measured initial radionuclide concentrations (µg/L) in synthetic TCU water

Test ID	Test Condition	Sr	Tc-99	I	Cs	Sm	Re	Np-237	U-238	Pu-242
A	Atmospheric	3,786±3.39	9.88±0.02	12,252±28.3	1,166±7.92	38.9±2.10	163±0.45	207±0.34	1,252±0.57	0.106±0.0004
B	1% O_2	4,720±41.9	12.7±0.06	20,788±73.5	1,483±11.3	5.48±0.11	211±1.19	266±3.73	1,114±19.2	0.135±0.003
C	0.1% O_2	4,601±0.00	12.1±0.01	18,152±67.9	1,434±2.26	56.3±3.76	200±0.40	256±2.66	1,549±11.9	0.134±0.002
D	11 ppm $FeCl_2$	3,149±24.3	8.39±0.04	1,896±301	957±10.8	27.9±38.5	141±0.74	98.6±33.1	962±33.9	0.037±0.042
E	24 ppm Na_2S	3,174±215	8.54±0.57	946±46.4	1,018±22.6	12.3±15.2	180±32.8	190±44.3	1,374±314	0.107±0.007

[a] Average concentration (mol/L) in parentheses.

Table 3. Measured redox potential Eh (mV) in different treatments

Test ID	Alluvium/J-13			Devitrified tuff/J-13		Zeolitic tuff/TCU			Carbonate/LCA		
	J-13 Control [a]	Blank	Sorption	Blank	Sorption	Control	Blank	Sorption	Control	Blank	Sorption
A	362±13	368±4.8	312±9.9	341±11	338±10	357±6.1	340±5.7	319±5.7	345±4.5	353±1.5	335±4.2
B	207±0.14	205±0.64	206±2.0	201±2.4	203±2.0	186±0.215	191±0.35	187±1.2	195±2.8	204±0.4	195±0.4
C	(-50)±1.0	(-27)±2.8	(-31)±1.1	(-41)±0.21	(-22)±0.31	29.4±0.64	(-8.3)±0.21	(-25)±0.36	(-35)±0.64	(-34)±1.6	(-22)±1.4
D	(-55)±9.9	(-83)±0.07	(-82)±1.0	(-82)±0.78	(-70)±1.4	(-98)±1.3	(-102)±2.8	(-95)±0.60	(-54)±2.5	(-90)±0.14	(-82)±0.67
E	(-50)±1.0	(-47)±1.8	(-63)±6.5	(-56)±2.4	(-59)±2.7	(-52)±0.78	(-69)±0.21	(-73)±0.38	(-52)±0.14	(-59)±2.2	(-68)±0.85

[a] The alluvium/J-13 control is also applicable for devitrified tuff/J-13 treatment.

Table 4. Measured pH values in different treatments

Test ID	Alluvium/J-13			Devitrified tuff/J-13		Zeolitic tuff/TCU			Carbonate/LCA		
	J-13 Control	Blank	Sorption	Blank	Sorption	Control	Blank	Sorption	Control	Blank	Sorption
A	7.63±0.27	7.89±0.01	7.84±0.04	8.09±0.13	7.89±0.09	8.02±0.06	7.91±0.08	7.89±0.03	8.01±0.08	7.69±0.13	7.84±0.09
B	8.50±0.34	8.76±0.02	8.48±0.03	9.08±0.09	8.32±0.03	8.98±0.02	9.27±0.04	9.01±0.01	8.05±0.04	9.26±0.06	8.59±0.02
C	8.72±0.15	8.08±0.02	8.70±0.06	9.38±0.04	8.66±0.06	8.95±0.20	8.30±0.03	9.04±0.04	9.64±0.03	9.35±0.14	8.89±0.23
D	7.79±0.04	8.97±0.09	8.89±0.03	8.57±0.08	8.51±0.06	9.54±0.01	9.66±0.03	9.63±0.08	9.36±0.10	9.50±0.24	9.15±0.03
E	8.40±0.05	9.11±0.17	9.01±0.02	9.50±0.05	8.75±0.05	9.68±0.01	9.85±0.01	9.72±0.01	8.54±0.11	9.51±0.14	9.28±0.04

Table 5. Measured iron concentrations (µg/L) in 0.2-µm filtrate in different treatments

Test ID	Alluvium/J-13			Devitrified tuff/J-13		Zeolitic tuff/TCU			Carbonate/LCA		
	J-13 Control	Blank	Sorption	Blank	Sorption	Control	Blank	Sorption	Control	Blank	Sorption
A	ND[a]	1038±1520	ND	1414±221	557±435	ND	27,752±5,894	26,328±4,882	ND	ND	106±36
B	ND	703±957	15.0±5.7	98.5±7.2	260±347	ND	5,545±4,139	4,465±3,050	ND	6.94±5.00	12.4±21.6
C	160±118	219±32.7	32.1±20.4	639±634	108±46.3	ND	123	3,539±3,136	ND	16.0±10.2	6.47±11.6
D[b]	891±1193	90.0±60.4	5.65±4.65	230±86	279±149	958±1,371	2,185±1,624	1,307±1,330	187±224	ND	171±254
E	ND	865±489	9.84±13.7	199±74.0	82.5±20.8	ND	4,734±491	5,475±4,227	27.3±17.7	ND	33.5±5.56

[a] ND: not detected; below the detection limit of about 5 µg/L.

[b] "11 ppm" $FeCl_2$ was added into both background and tracer sorption solutions used in Test D. Measured Fe^{2+} concentrations in the control samples are in the range of 0.2 to 1 ppm, which is consistent with the excepted dissolved Fe^{2+} concentrations from Geochemist's Workbench; the Fe^{2+} in solution is controlled by the solubility of $FeCO_3$ and/or $Fe(OH)_2$.

Figure Captions

Figure 1 Eh-pH diagram drawn at 25 °C and an equilibrium activity of 10^{-11} for technetium; stability fields are shown only for the aqueous species. Diagram was produced using the "thermo" database in the Geochemist's Workbench (version 6.0). Hatched areas are the measured Eh-pH region for Tests A-E conducted in this work.

Figure 2 Eh-pH diagrams drawn at 25 °C and a species activity of 10^{-13} M for (a) uranium, (b) neptunium and (c) plutonium in J-13 water; stability fields are shown only for the aqueous species.

Figure 3 Expected dominant oxidation states of the radionuclides as a function of standard redox potential under pH 7 in J-13 water at equilibrium with atmospheric CO_2. Arrows at the top of the figure shows the expected redox potentials for common redox couples in the groundwater. This figure was modified from Banaszak et al [36].

Figure 4 Change of solution Eh in response to the gas composition (99% Ar and 1% CO_2) inside the glove box; (A) three different background solutions; and (B) J-13 water and devitrified tuff (*tuff a* and *tuff b* are duplicate runs inside centrifuge tubes).

Figure 5 Change of (a) Sr and (b) Cs K_d values under six different redox conditions for different aquifer materials.

Figure 6 Change of ^{99}Tc K_d values under six different redox conditions for different aquifer materials (negative K_d values were plotted as 0.1 mL/g).

Figure 7 Change of iodine K_d values under six different redox conditions for different aquifer materials (negative K_d values wre plotted as 0.1 mL/g).

Figure 8 Change of ^{237}Np K_d values under six different redox conditions for different aquifer materials.

Figure 9 Change of (a) U and (b) ^{242}Pu K_d values under six different redox conditions for different aquifer materials; negative K_d values were plotted as 0.1 mL/g.

Figure 10 Stability fields of Np species in Eh-pH diagram for LCA waters.

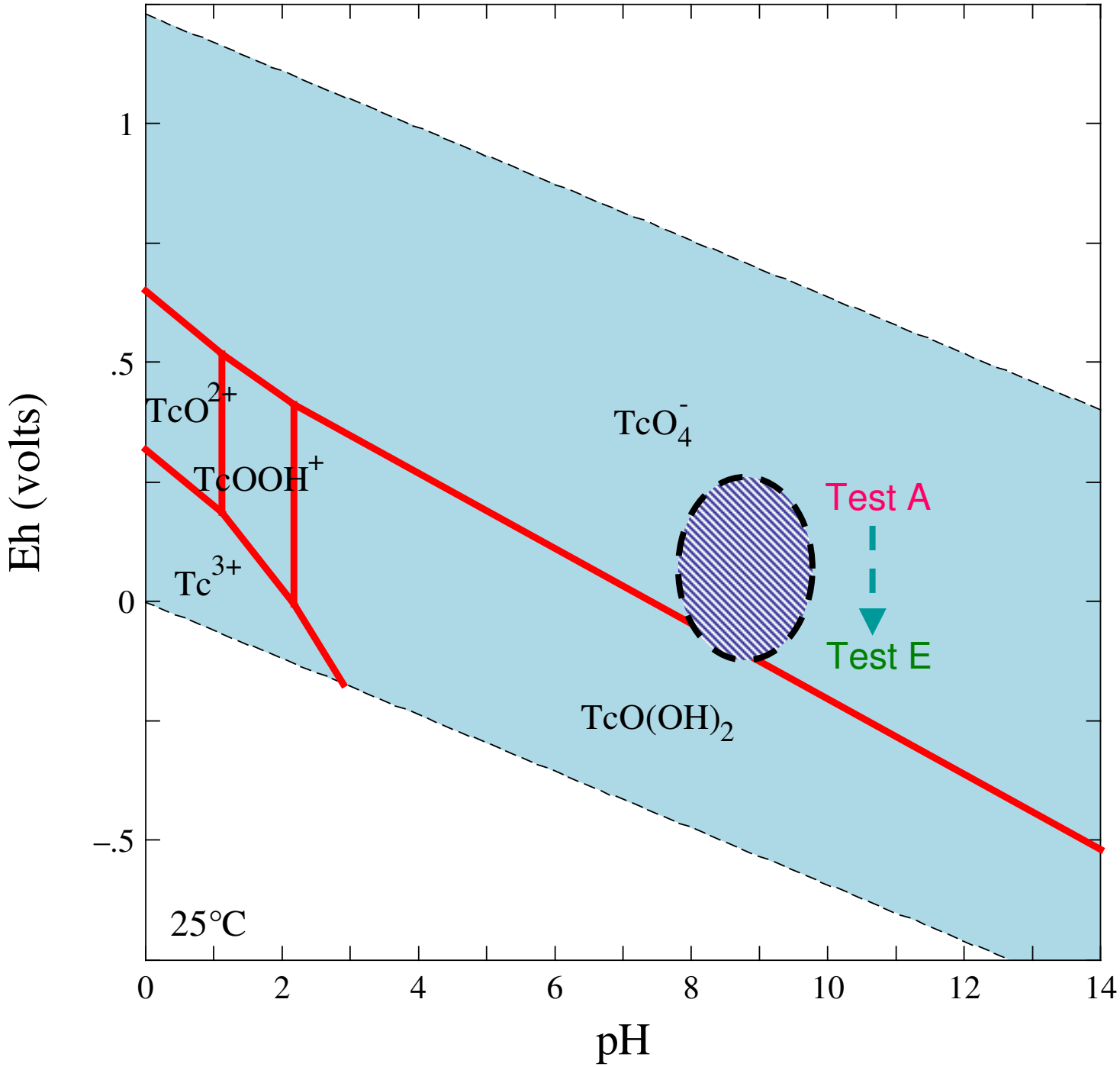
Eh (volts)
1
.5
0
–.5
0
2
4
6
8
10
12
14
pH
TcO2+
TcOOH+
Tc3+
TcO4-
TcO(OH)2
Test A
Test E
25°C

Figure 1

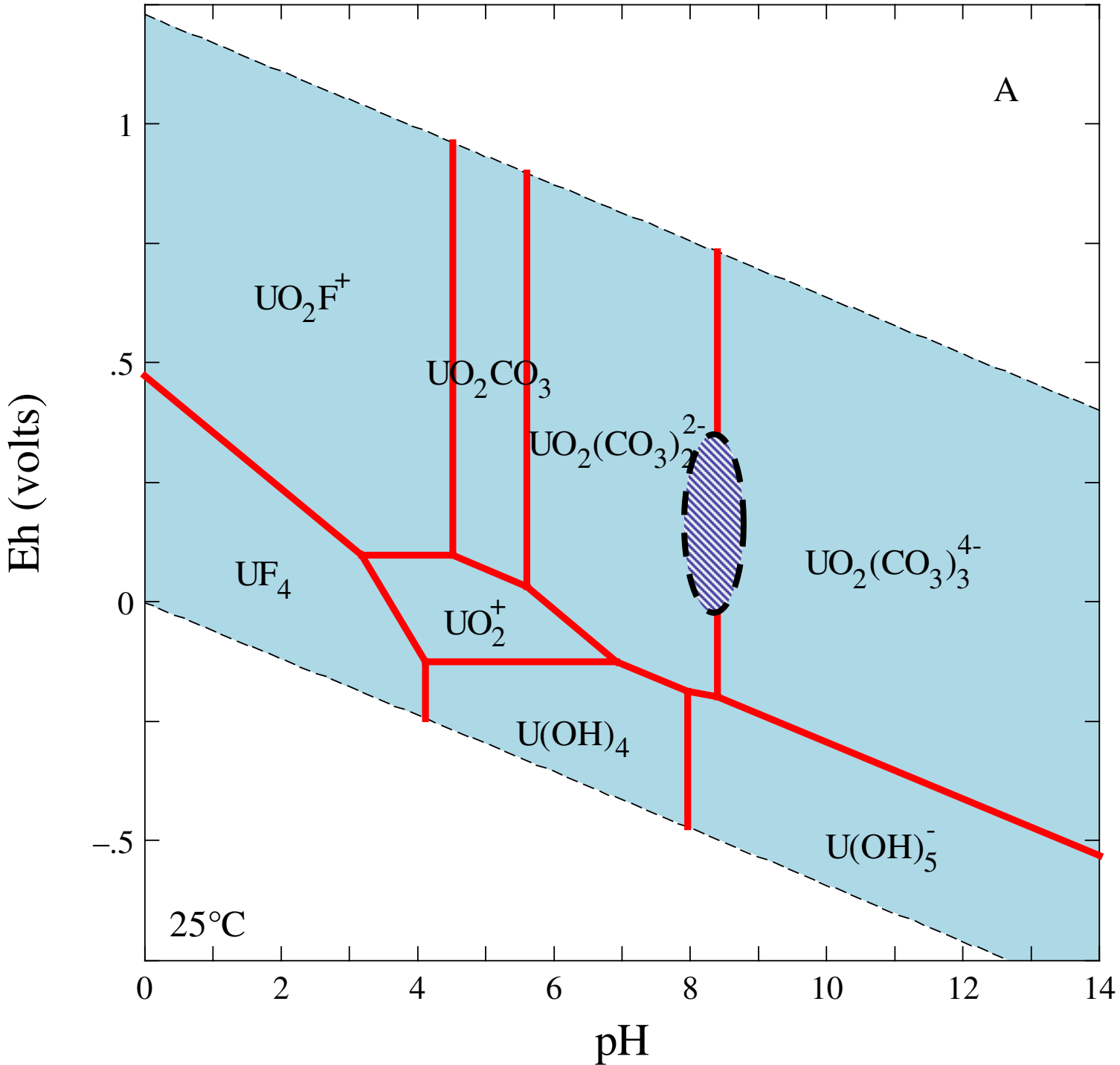
A
UO_2F^+
UO_2CO_3
$UO_2(CO_3)_2^{2-}$
UF_4
UO_2^+
$UO_2(CO_3)_3^{4-}$
$U(OH)_4$
$U(OH)_5^-$
25°C
Eh (volts)
1
.5
0
–.5
0
2
4
6
8
10
12
14
pH

Figure 2

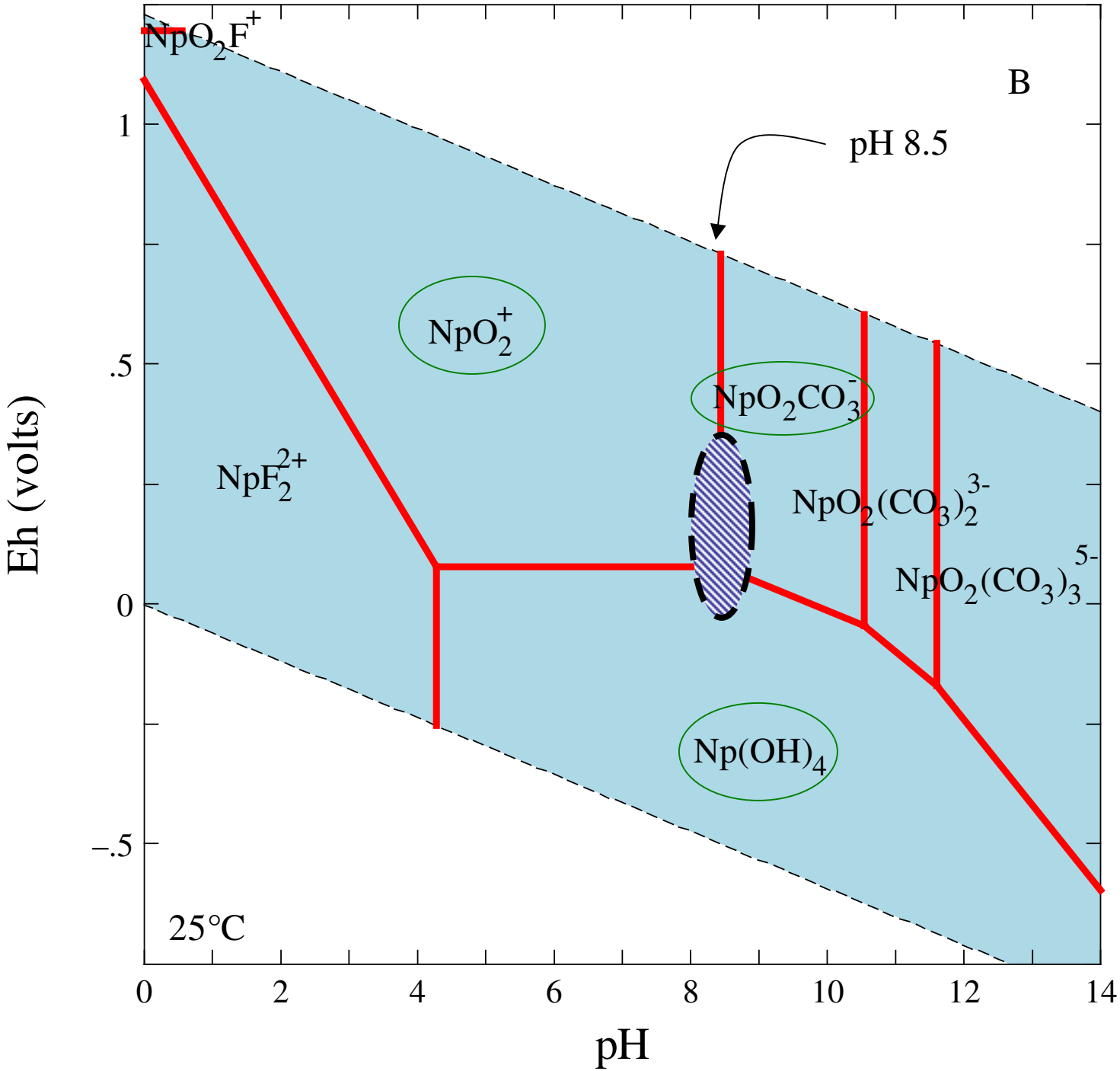
NpO2F+
B
pH 8.5
NpO2+
NpO2CO3-
NpF2 2+
NpO2(CO3)2 3-
NpO2(CO3)3 5-
Np(OH)4
25°C
Eh (volts)
1
.5
0
–.5
0
2
4
6
8
10
12
14
pH

Figure 3

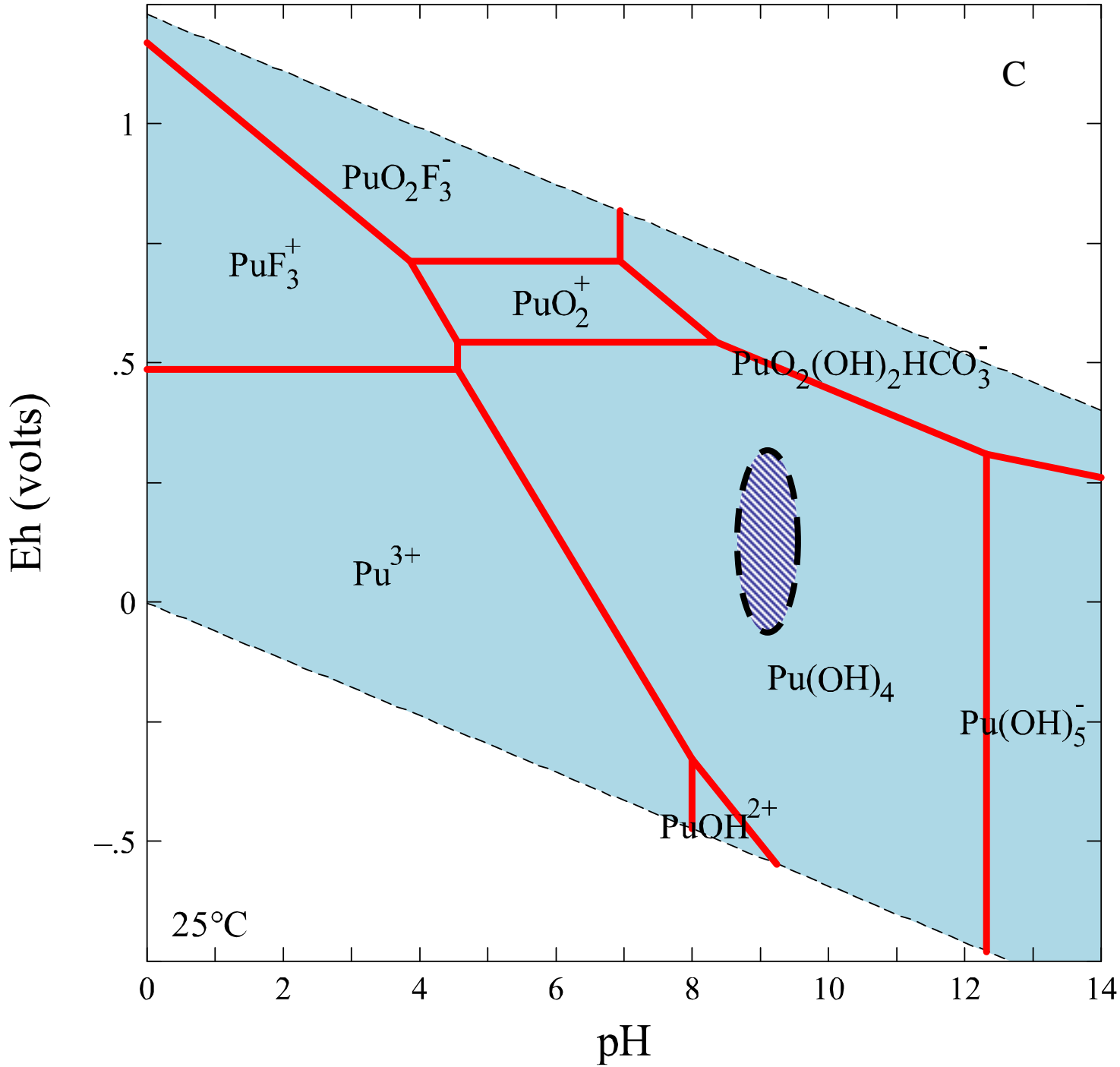
C
$PuO_2F_3^-$
PuF_3^+
PuO_2^+
$PuO_2(OH)_2HCO_3^-$
Pu^{3+}
$Pu(OH)_4$
$Pu(OH)_5^-$
$PuOH^{2+}$
25°C
Eh (volts)
pH
1
.5
0
–.5
0
2
4
6
8
10
12
14

Figure 4

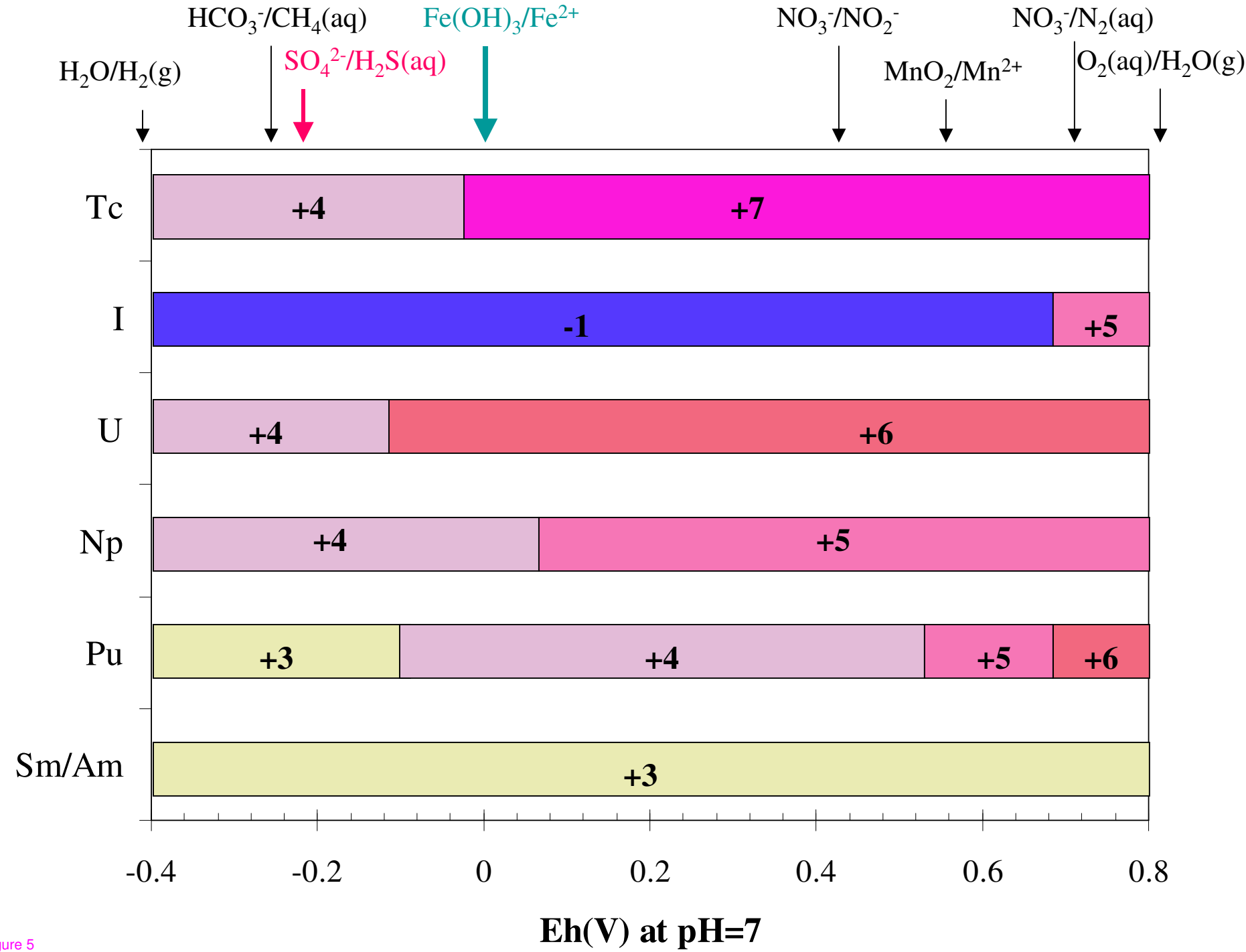
$HCO_3^-/CH_4(aq)$
$Fe(OH)_3/Fe^{2+}$
NO_3^-/NO_2^-
$NO_3^-/N_2(aq)$
$H_2O/H_2(g)$
$SO_4^{2-}/H_2S(aq)$
MnO_2/Mn^{2+}
$O_2(aq)/H_2O(g)$
Tc
+4
+7
I
-1
+5
U
+4
+6
Np
+4
+5
Pu
+3
+4
+5
+6
Sm/Am
+3
-0.4
-0.2
0
0.2
0.4
0.6
0.8
Eh(V) at pH=7

Figure 5

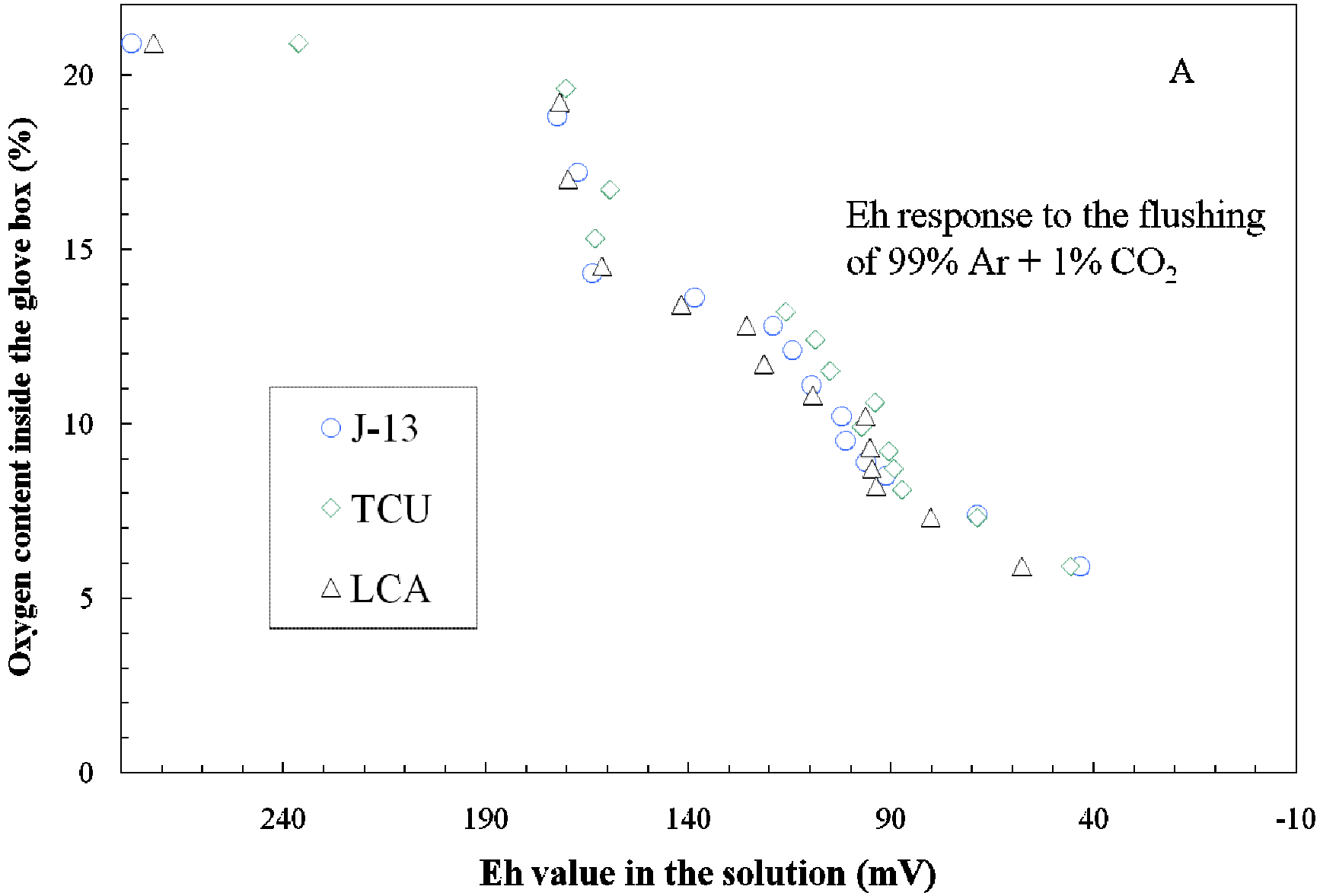
A
Eh response to the flushing
of 99% Ar + 1% CO_2
J-13
TCU
LCA
Oxygen content inside the glove box (%)
0
5
10
15
20
240
190
140
90
40
-10
Eh value in the solution (mV)

Figure 6

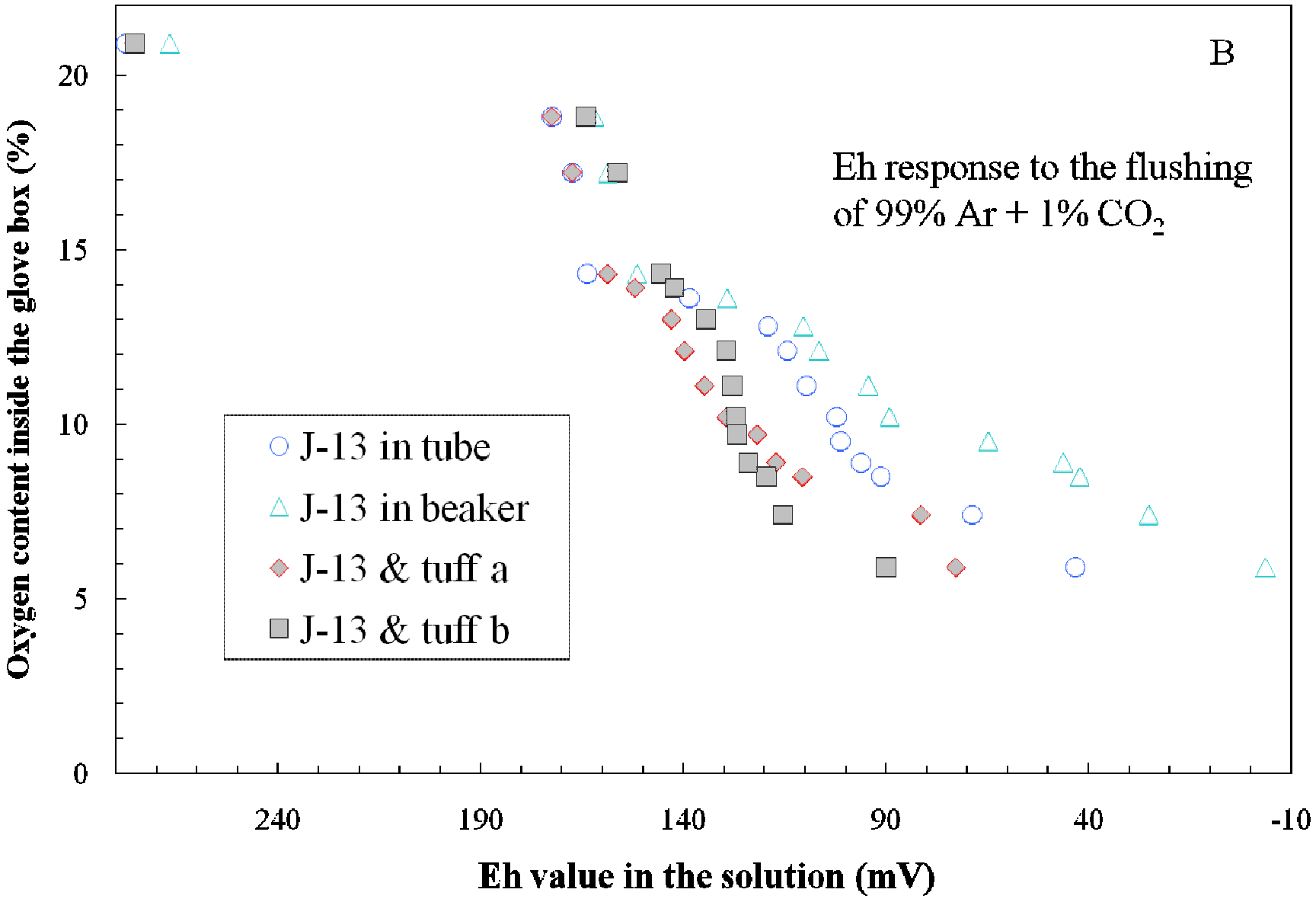
B
Eh response to the flushing of 99% Ar + 1% CO_2
J-13 in tube
J-13 in beaker
J-13 & tuff a
J-13 & tuff b
Oxygen content inside the glove box (%)
0
5
10
15
20
240
190
140
90
40
-10
Eh value in the solution (mV)

Figure 7

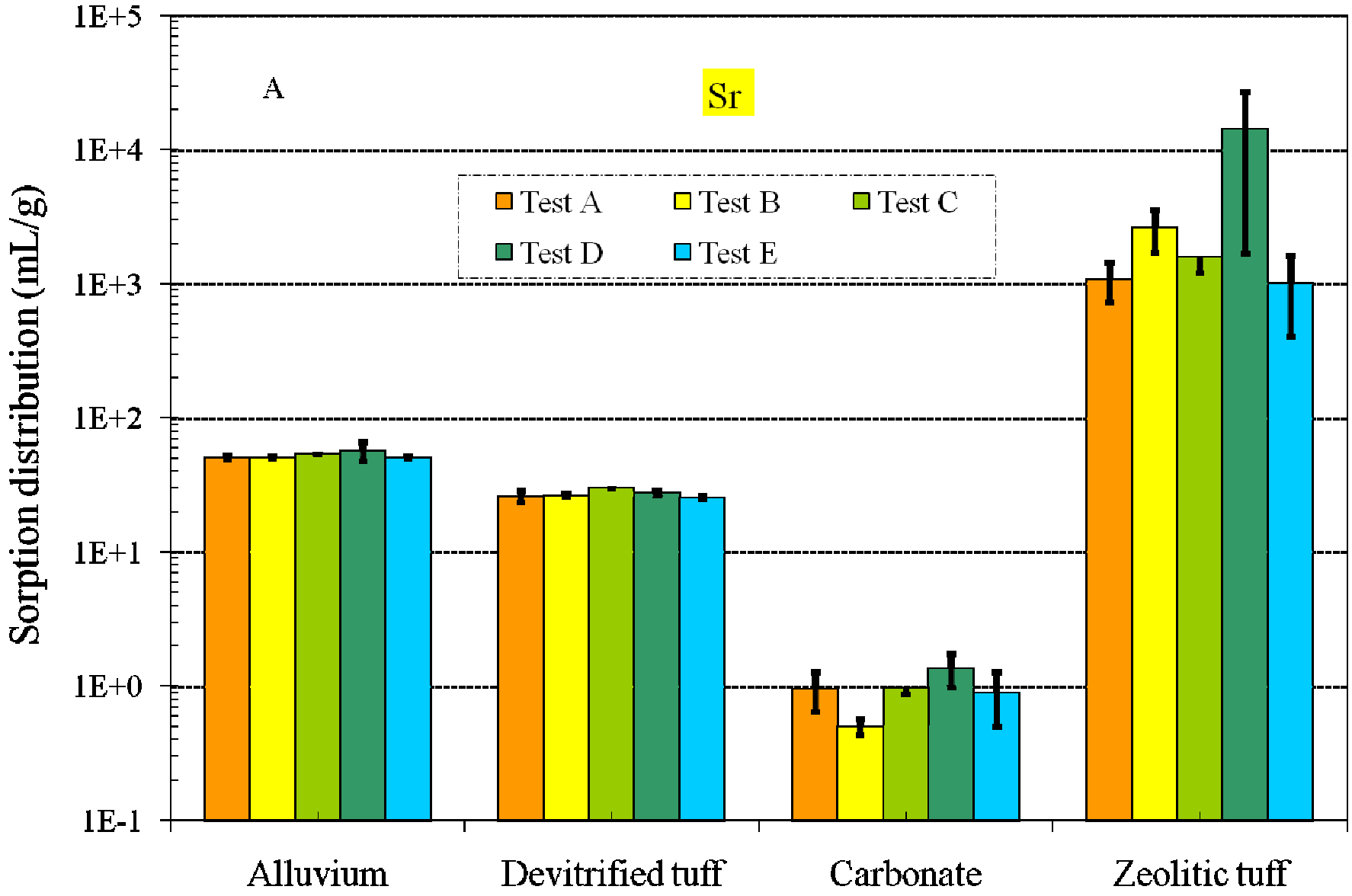
A
Sr
Test A
Test B
Test C
Test D
Test E
Sorption distribution (mL/g)
1E+5
1E+4
1E+3
1E+2
1E+1
1E+0
1E-1
Alluvium
Devitrified tuff
Carbonate
Zeolitic tuff

Figure 8

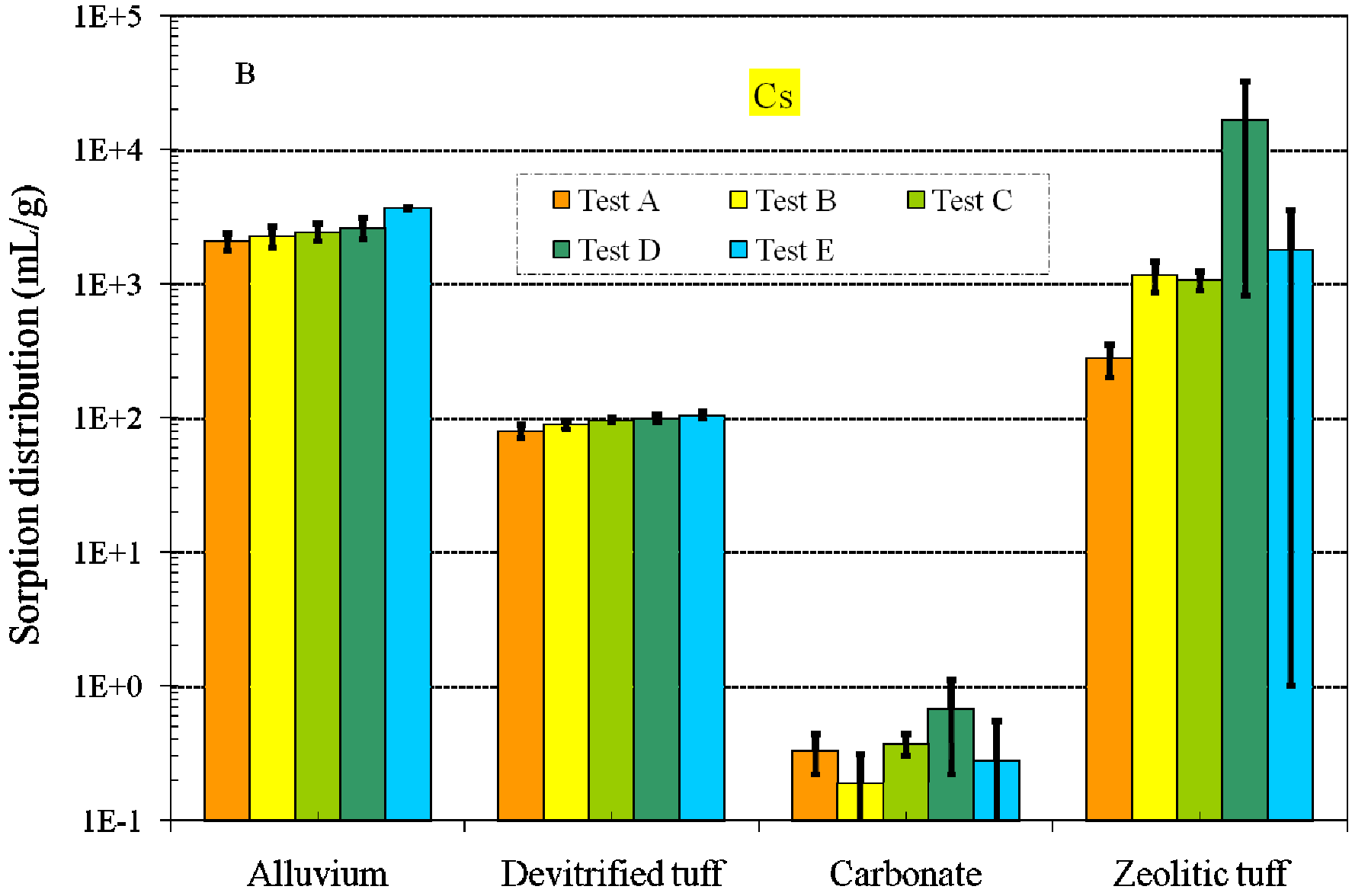
B
Cs
Test A
Test B
Test C
Test D
Test E
Sorption distribution (mL/g)
1E+5
1E+4
1E+3
1E+2
1E+1
1E+0
1E-1
Alluvium
Devitrified tuff
Carbonate
Zeolitic tuff

Figure 9

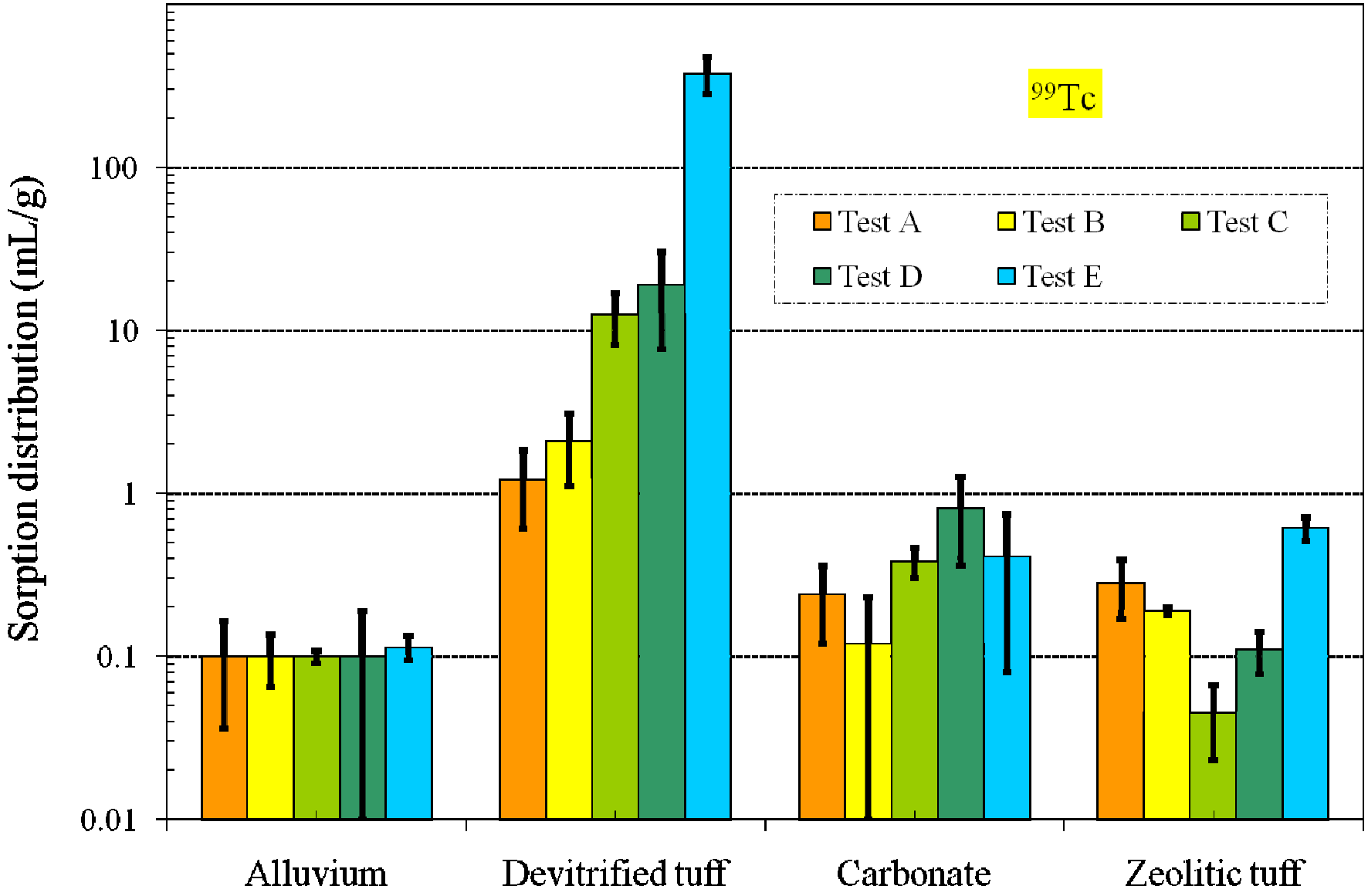
^{99}Tc
Test A
Test B
Test C
Test D
Test E
Sorption distribution (mL/g)
100
10
1
0.1
0.01
Alluvium
Devitrified tuff
Carbonate
Zeolitic tuff

Figure 10

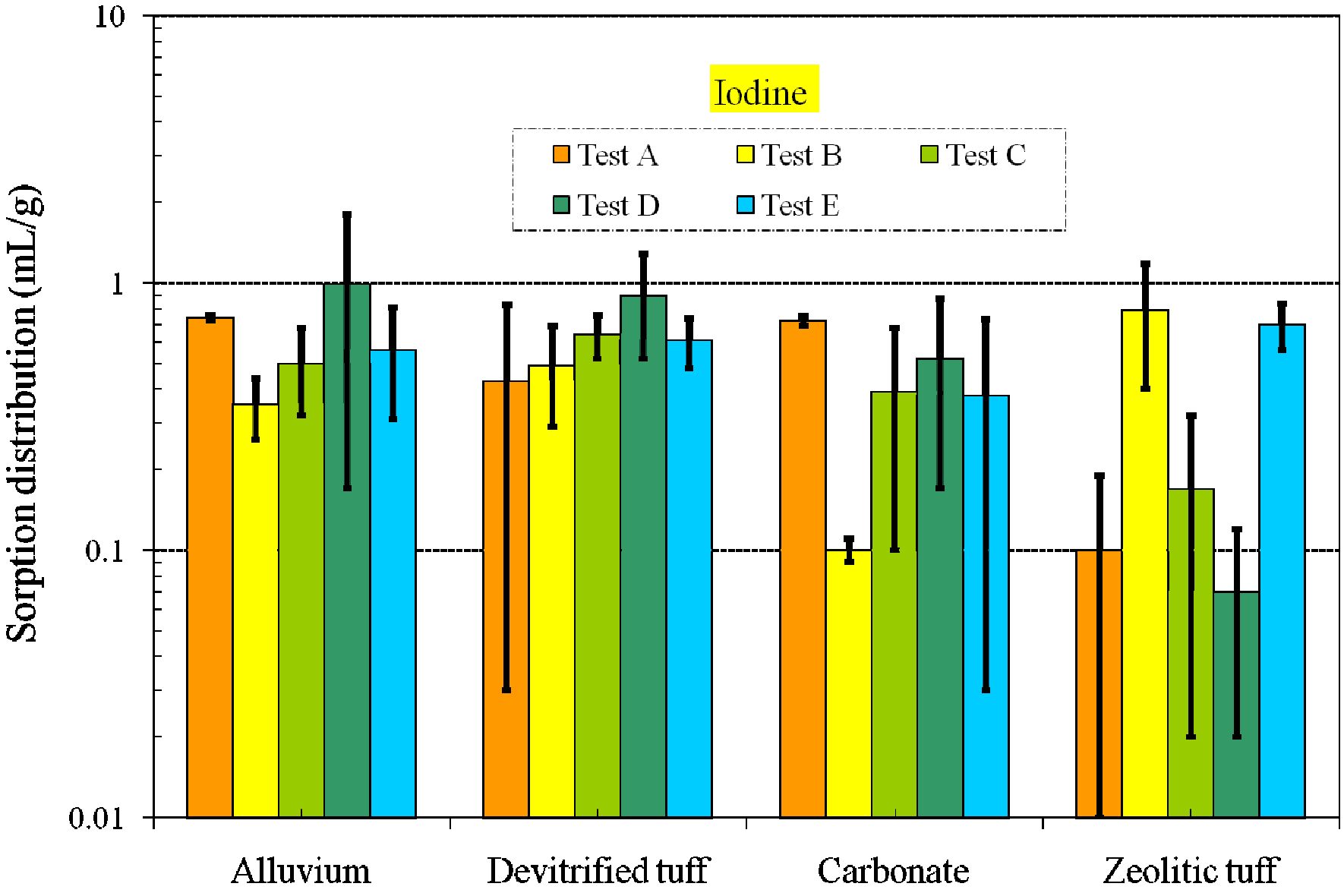
Iodine
Test A
Test B
Test C
Test D
Test E
Sorption distribution (mL/g)
10
1
0.1
0.01
Alluvium
Devitrified tuff
Carbonate
Zeolitic tuff

Figure 11

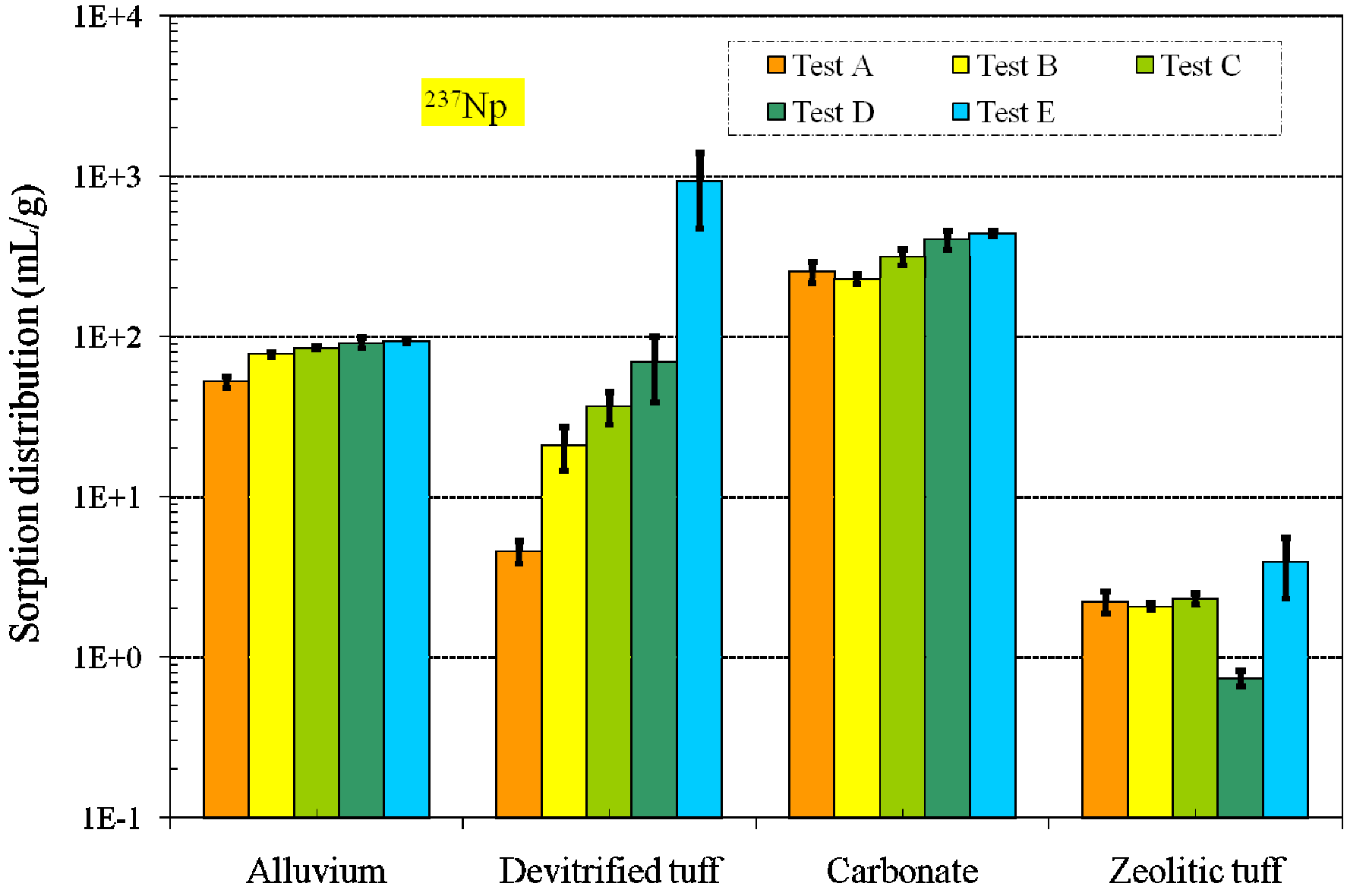
1E+4
1E+3
1E+2
1E+1
1E+0
1E-1
Sorption distribution (mL/g)
^{237}Np
Test A
Test B
Test C
Test D
Test E
Alluvium
Devitrified tuff
Carbonate
Zeolitic tuff

Figure 12

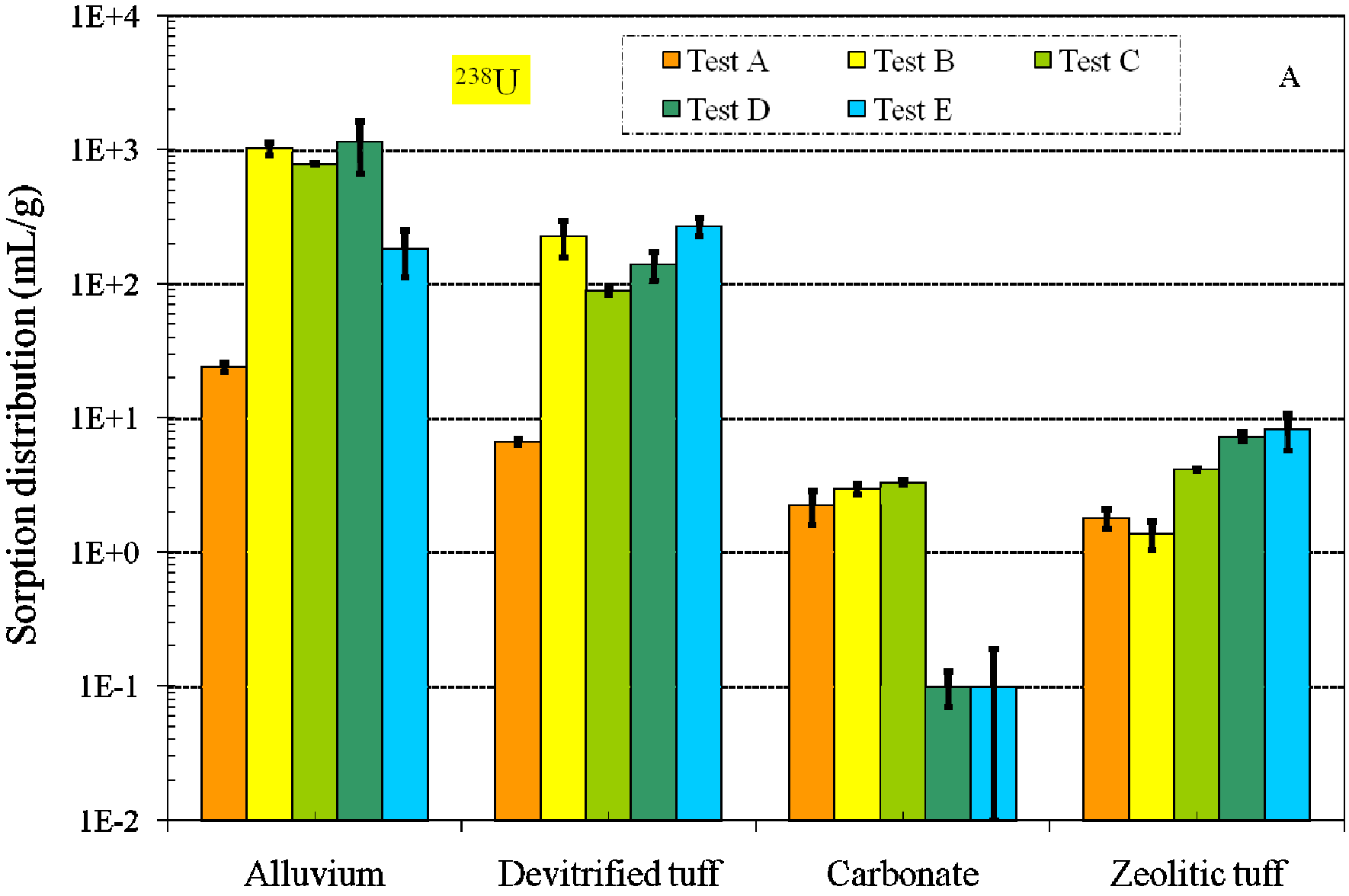
1E+4
1E+3
1E+2
1E+1
1E+0
1E-1
1E-2
Sorption distribution (mL/g)
238U
Test A
Test B
Test C
Test D
Test E
A
Alluvium
Devitrified tuff
Carbonate
Zeolitic tuff

Figure 13

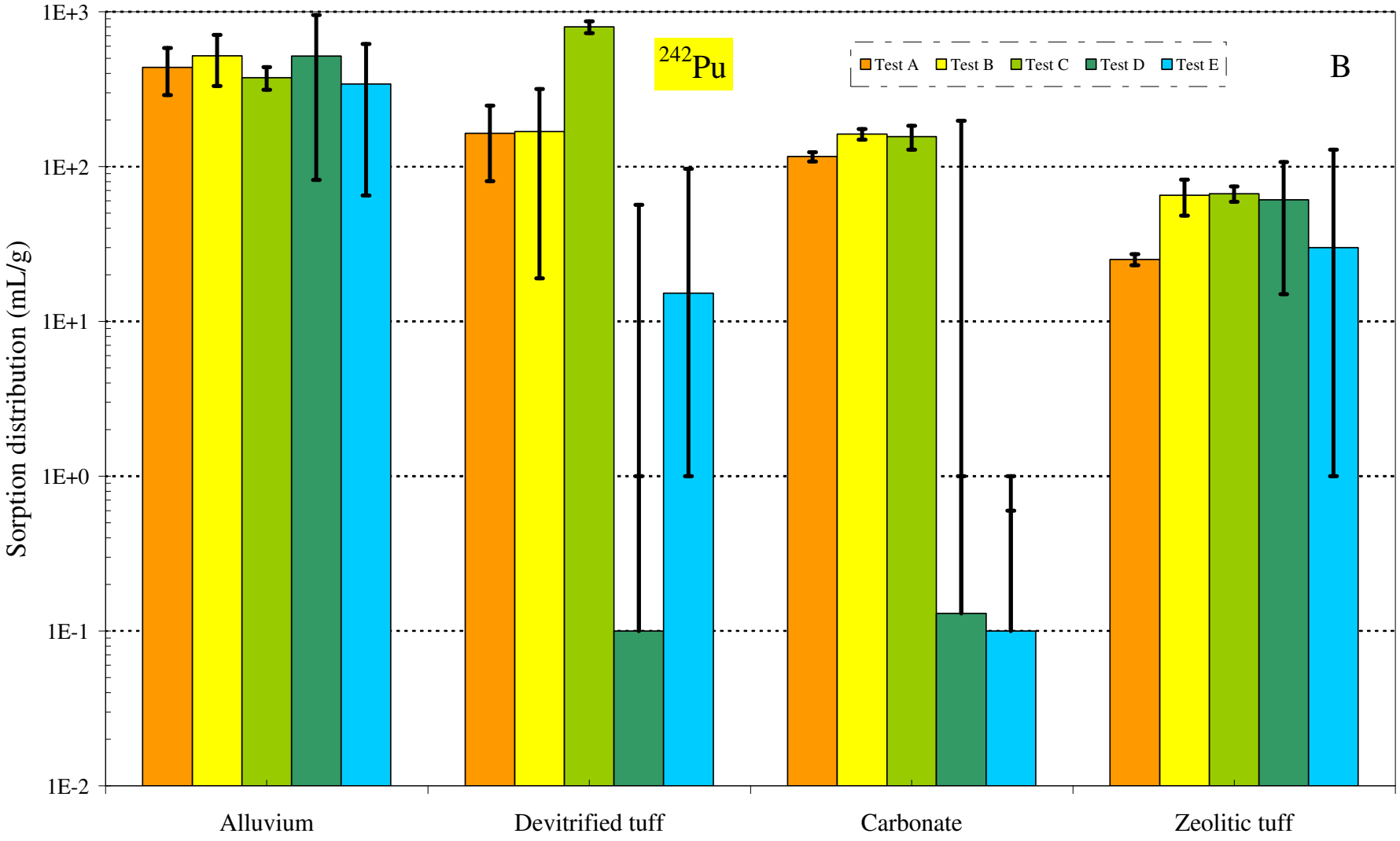
1E+3
1E+2
1E+1
1E+0
1E-1
1E-2
Sorption distribution (mL/g)
242Pu
Test A
Test B
Test C
Test D
Test E
B
Alluvium
Devitrified tuff
Carbonate
Zeolitic tuff

Figure 14

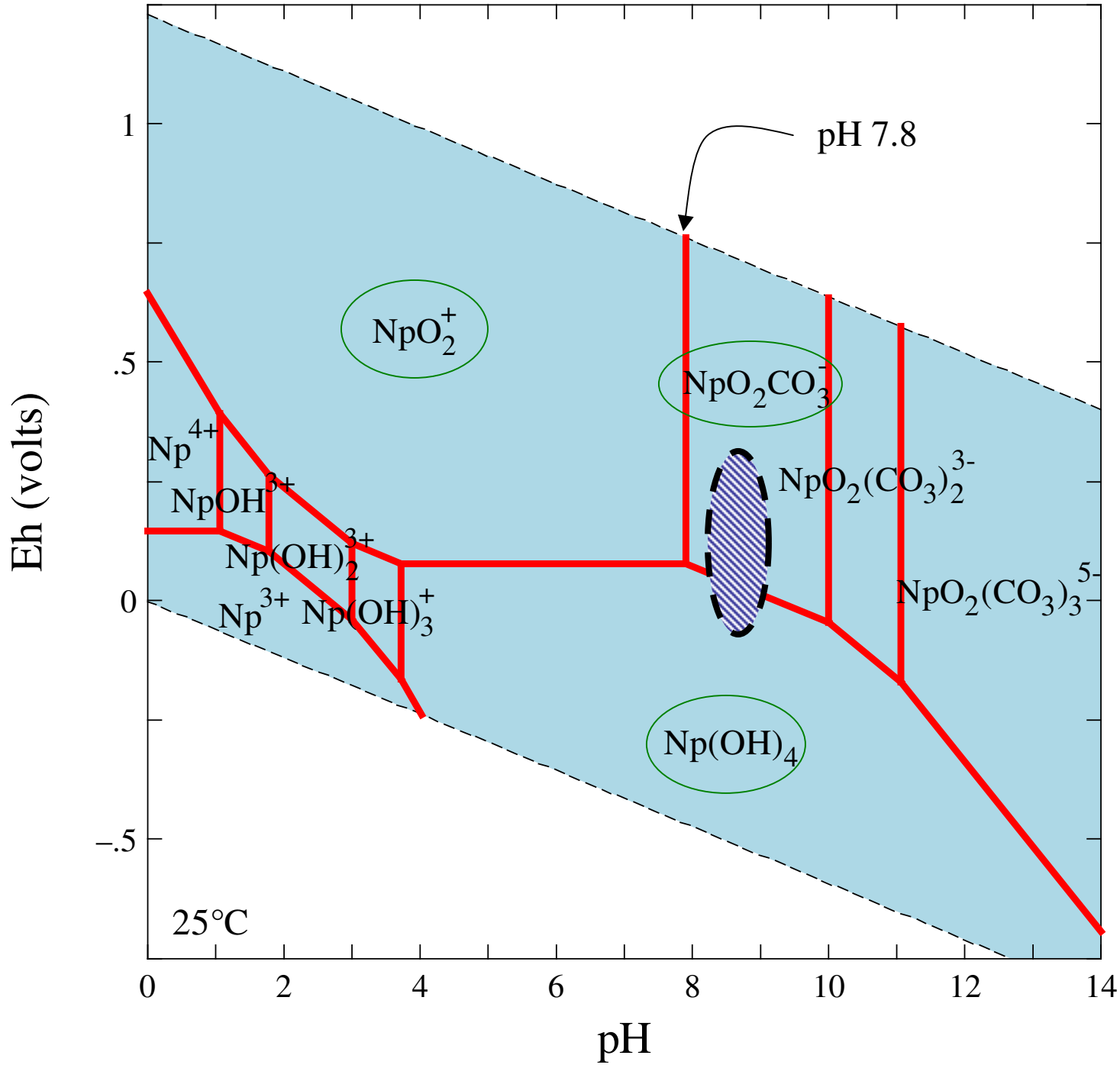
pH 7.8
NpO_2^+
$NpO_2CO_3^-$
Np^{4+}
$NpOH^{3+}$
$Np(OH)_2^{3+}$
Np^{3+}
$Np(OH)_3^+$
$NpO_2(CO_3)_2^{3-}$
$NpO_2(CO_3)_3^{5-}$
$Np(OH)_4$
25°C
Eh (volts)
pH
1
.5
0
–.5
0
2
4
6
8
10
12
14

Figure 15